# Sensitivity Analysis of Added Power of Ships in Seaway


## Ricardo dos Santos Ferreira


**Master Thesis**

presented in partial fulfillment
of the requirements for the double degree:
“Advanced Master in Naval Architecture” conferred by University of Liege
"Master of Sciences in Applied Mechanics, specialization in Hydrodynamics, Energetics and Propulsion” conferred by Ecole Centrale de Nantes

developed at University of Rostock, Rostock
in the framework of the

**“EMSHIP”**
**Erasmus Mundus Master Course**
**in “Integrated Advanced Ship Design”**


EMJMD 159652 – Grant Agreement 2015-1687


Supervisor: Prof. Robert Bronsart, University of Rostock

Reviewer: Dr. Vladimir Shigunov, DNV GL SE, Hamburg
Prof. Léonard Domnisoru, University of Galati

Rostock, February 2018

# DECLARATION OF AUTHORSHIP

I, Ricardo dos Santos Ferreira, declare that this thesis and the work presented in it are my own and has been generated by me as the result of my own original research.

*Sensitivity Analysis of Added Power of Ships in Seaway.*

I confirm that:

1. This work was done wholly or mainly while in candidature for a research degree at this University;

2. Where any part of this thesis has previously been submitted for a degree or any other qualification at this University or any other institution, this has been clearly stated;

3. Where I have consulted the published work of others, this is always clearly attributed;

4. Where I have quoted from the work of others, the source is always given. With the exception of such quotations, this thesis is entirely my own work;

5. I have acknowledged all main sources of help;

6. Where the thesis is based on work done by myself jointly with others, I have made clear exactly what was done by others and what I have contributed myself;

7. Either none of this work has been published before submission, or parts of this work have been published as: [please list references below]:

8. I cede copyright of the thesis in favor of the University of Rostock and University of Liège.

Signed:

Date:

# ABSTRACT

The aim of this master thesis is to identify most important parameters for the prediction of added power of a ship in waves. Such study enables a better understanding of the added power in waves problem, by allowing one to identify which parameters play a more important role in the final estimation. This study can contribute to the scientific community which is working on a precise numerical solution for this problem by providing a better comprehension on the problem regarding parameters that should be given more effort to achieve a finer tuning. This research is based on a large amount of full-scale container ship data where a comparison between measurements and numerically calculated added power of a ship in waves can be performed. The numerical approach is based on the method proposed by Shigunov V. (2017).

# TABLE OF CONTENTS

DECLARATION OF AUTHORSHIP iii
ABSTRACT v
TABLE OF CONTENTS vii
LIST OF FIGURES ix
LIST OF TABLES xi
1. INTRODUCTION 1
1.1. Motivation 1
1.2. Literature Review 2
1.2.1. Prediction of Added Power in Seaway by Numerical Simulation – [1] 2
1.2.2. A Study of Methods to Predict Added Resistance in Waves – [2] 2
1.2.3. A Comparison of Different Methods for Added Resistance Prediction – [3] 2
1.2.4. Uncertainties Related to the Estimation of Added Resistance of a Ship in Waves – [4] 2
1.2.5. Experimental Study on Added Resistance and Unsteady Pressure Distribution in Following Waves – [5] 2
1.2.6. Estimating Added Power in Waves for Ships Through Analysis of Operational Data – [6] 3
2. Investigation Method 4
2.1. Data preparation 5
2.2. Environmental Conditions 6
2.3. Hydrodynamic Model 6
2.4. GL Power Software 7
2.5. Sensitivity Study 8
3. POST PROCESSING OF MESUREMENTS 9
3.1. Environmental Conditions 9
3.1.1. Wind Information 9
3.1.2. Wave information 9
3.1.3. Ocean Current 10
3.2. Resulting Database 10
3.3. Environmental Data Consistency Check 11
4. ADDED POWER Calculation 12
4.1. GL Power Input Files 12

4.1.1. Calm-Water Reactions 12
4.1.2. Wind Force 14
4.1.3. Wave Drift Forces 14
4.1.4. Propeller Characteristics 15
4.1.5. Rudder Forces 15
4.1.6. GL Power Solution Method 16
4.2. Ship Added Power Estimation 17
4.3. Added Power Script Development 18
5. RESULTS AND ANALYSIS 19
5.1. Added Power 19
5.2. Total Power 23
5.3. Ratio of Computed to Measured Total Power 28
5.4. Measured Total Power vs Calculated Added Power 33
5.5. Measured Total Power X Calculated Added Power (By Classes) 38
5.5.1. Average Results Segregated by Speed 40
5.5.2. Average Results Segregated by Shaft Power 44
6. CONCLUSION AND OUTLOOK 48
7. FUTURE WORK AND FURTHER INVESTIGATIONS 51
8. ACKNOWLEDGEMENTS 52
9. REFERENCES 53

# LIST OF FIGURES

Figure 1 - Schematic of steps taken. ..... 5
Figure 2 – Filtered loading conditions. ..... 6
Figure 3 – Coordinate system (picture from GL Power manual). ..... 7
Figure 4 - GL Power input example. ..... 12
Figure 5 - Calm-water coefficients input file. ..... 12
Figure 6 - Histogram with mean draft. ..... 13
Figure 7 – Wave drift forces input. ..... 14
Figure 8 - Wave drift forces envelope conditions. ..... 15
Figure 9 - Total added power due to wind (x-axis) vs. measured (y-axis) – Case 2. ..... 19
Figure 10 - Total added power due to wave (x-axis) vs. measured (y-axis) – Case 3. ..... 20
Figure 11 - Total added power due to current (x-axis) vs. measured (y-axis) – Case 4. ..... 20
Figure 12 - Total added power due to wind & wave (x-axis) vs. measured (y-axis) – Case 5. 21
Figure 13 - Total added power due to wind & current (x-axis) vs. measured (y-axis) – Case 6. ..... 21
Figure 14 - Total added power due to wave & current (x-axis) vs. measured (y-axis) – Case 7. ..... 22
Figure 15 - Total added power computed (x-axis) vs. measured (y-axis) – Case 8. ..... 22
Figure 16 – Total power computed (y-axis) vs. measured (x-axis) – Case 8. ..... 23
Figure 17 – Theoretical comparison of calm water power (Case 1, y-axis) vs. total calculated power. ..... 24
Figure 18 – Theoretical comparison of wind power (Case 2, y-axis) vs. total calculated power. ..... 25
Figure 19 – Theoretical comparison of wave power (Case 3, y-axis) vs. total calculated power. ..... 25
Figure 20 – Theoretical comparison of current power (Case 4, y-axis) vs. total calculated power. ..... 26
Figure 21 – Theoretical comparison of wind & wave power (Case 5, y-axis) vs. total calculated power. ..... 26
Figure 22 – Theoretical comparison of wind & current power (Case 6, y-axis) vs. total calculated power. ..... 27
Figure 23 – Theoretical comparison of wave & current power (Case 7, y-axis) vs. total calculated power. ..... 27

Figure 24 – Measured total power (x-axis) vs. calm-water power ratio (Case 1, y-axis). ..... 29
Figure 25 – Measured total power (x-axis) vs. wind power ratio (Case 2, y-axis). ..... 29
Figure 26 – Measured total power (x-axis) vs. wave power ratio (Case 3, y-axis)..... 30
Figure 27 – Measured total power (x-axis) vs. current power ratio (Case 4, y-axis)..... 30
Figure 28 – Measured total power (x-axis) vs. wind & wave power ratio (Case 5, y-axis). ... 31
Figure 29 – Measured total power (x-axis) vs. wind & current power ratio (Case 6, y-axis).. 31
Figure 30 – Measured total power (x-axis) vs. wave & current power ratio (Case 7, y-axis). 32
Figure 31 – Measured total power (x-axis) vs. total power computed ratio (Case 8, y-axis). . 32
Figure 32 – Measured total power (x-axis) vs. computed calm-water power (Case 1, y-axis). ..... 33
Figure 33 – Measured total power (x-axis) vs. computed wind power (Case 2, y-axis)..... 34
Figure 34 – Measured total power (x-axis) vs. computed wave power (Case 3, y-axis). ..... 34
Figure 35 – Measured total power (x-axis) vs. computed current power (Case 4, y-axis). ..... 35
Figure 36 – Measured total power (x-axis) vs. computed wind & wave power (Case 5, y-axis). ..... 35
Figure 37 – Measured total power (x-axis) vs. computed wind & current power (Case 6, y-axis). ..... 36
Figure 38 – Measured total power (x-axis) vs. computed wave & current power (Case 7, y-axis). ..... 36
Figure 39 – Measured total power (x-axis) vs. computed total power (Case 8, y-axis). ..... 37
Figure 40 – Speed histogram. ..... 39
Figure 41 – Shaft power histogram. ..... 39
Figure 42 – Cases 1 to 4 - distributed over ship speed. ..... 40
Figure 43 – Cases 5 to 8 – distributed over speed. ..... 41
Figure 44 – Cases 1 to 4 ratio - distributed over speed. ..... 42
Figure 45 – Cases 5 to 8 ratio - distributed over speed. ..... 43
Figure 46 – Cases 1 to 4 - distributed over shaft power. ..... 44
Figure 47 – Cases 5 to 8 - Distributed over shaft power. ..... 45
Figure 48 – Cases 1 to 4 ratio - distributed over shaft power. ..... 46
Figure 49 – Cases 5 to 8 Ratio - Distributed over shaft power. ..... 47

# LIST OF TABLES

Table 1 - Studied cases. ..... 17
Table 2 – Slope $\theta$ and $R^2$ of theoretical comparison. ..... 28
Table 3 – Slope $\theta$ and $R^2$ of measured vs. calculated total power. ..... 37
Table 4 – Speed ranges. ..... 38
Table 5 – Shaft power ranges. ..... 38
Table 6 – Cases 1 to 4 average power by speed range. ..... 40
Table 7 – Cases 5 to 8 average power by speed range. ..... 41
Table 8 – Cases 1 to 4 average ratio by speed range. ..... 42
Table 9 – Cases 5 to 8 average ratio by speed range. ..... 43
Table 10 – Cases 1 to 4 average power by shaft power range. ..... 44
Table 11 – Cases 5 to 8 average power by shaft power range. ..... 45
Table 12 – Cases 1 to 4 average ratio by shaft power range. ..... 46
Table 13 – Cases 5 to 8 average ratio by shaft power range. ..... 47
Table 14 – Percent difference of influencing parameters on cases 1 to 4 – speed range. ..... 49
Table 15 – Percent difference of influencing parameters on cases 5 to 8 – speed range. ..... 49
Table 16 – Percent difference of influencing parameters on cases 1 to 4 – shaft power range. ..... 49
Table 17 – Percent difference of influencing parameters on cases 5 to 8 – shaft power range. ..... 50

# 1. INTRODUCTION

## 1.1. Motivation

DNV GL SE Hamburg, Fluid Engineering Department of Advisory is an important player on the ship industry providing hydrodynamic advisory services to the external customers, internal rule development and approval. A shipping company has requested DNV GL to perform an assessment of the sufficiency of sea margin to fulfill contract requirements for four series of container ships with retrofitted bow and derated engine for slow-steaming operation. This was done using numerical method; to validate this method, the customer asked DNV GL to compare the results of this method with measurements for a series of eight sister container ships for a period of 7 ship-years and provided a database of such measurements.

Such study enables a better understanding of the added power in waves problem, by allowing one to identify most important factors. Certainly, this study can contribute to the scientific community which is working on a precise numerical solution for this problem by providing a better comprehension on the problem and identification of factors that should be given more effort to achieve a better accuracy.

Another positive impact would be on the performance monitoring of ships. In this case the performance is monitored and checked by converting the results from the operational condition to calm-water condition. A more accurate correction approach would lead to more realistic results.

Furthermore, a contribution on such topic can have a major importance to the industry, because ships are mainly designed and optimized for still water conditions. In this way, a contribution to this topic would enable the industry to enhance the sea margins commonly applied on design phase.

A large amount of full-scale container ship data is available to DNV GL which enables the development of a study where a comparison between a real measurements and numerical calculations of added power of a ship in waves can be performed. The main goal of the proposed topic is to try to investigate and identify the influence of each parameter that can affect the result of added power of the ship.

Lastly, this research contributed to DNV GL to keep developing a software tool with an automatic search, post-processing and filtering of environmental data (current, wind, waves) for given ship locations.

## 1.2. Literature Review

Below a list of reference publications on this subject and a brief description of their content.

### *1.2.1. Prediction of Added Power in Seaway by Numerical Simulation – [1]*

This paper was the basis for the bibliography research on this study. In this publication it is proposed a numerical method to predict added power in seaway. The proposed method combines wave and wind forces with calm-water reactions and forces from propulsion system and rudders. The numerical predictions are compared with full scale measurements.

### *1.2.2. A Study of Methods to Predict Added Resistance in Waves – [2]*

This reference is a master thesis where the author has made a research on the available methods to predict the added resistance of ships in waves. One of the useful outcomes for this research is the list of methods described in the work. Most of the methods were developed in 1970s, and have a good agreement with experimental results for head seas.

### *1.2.3. A Comparison of Different Methods for Added Resistance Prediction – [3]*

This reference, similarly to [2], compares different added resistance prediction methods. This comparison is done for a Ro-Ro/Pax ship. The main outcome is that after evaluating both analytical and statistical methods it was concluded that the statistical regressions should be updated by the new Ro-Ro/pax profile designs.

### *1.2.4. Uncertainties Related to the Estimation of Added Resistance of a Ship in Waves – [4]*

This work similarly to previous ones, compares different methods for assessing the added resistance of ships in waves. The uncertainty origins are analyzed and compared taking in consideration assumptions and simplifications on each method.

### *1.2.5. Experimental Study on Added Resistance and Unsteady Pressure Distribution in Following Waves – [5]*

This paper goal is to discuss the applicability of Enhanced Uniform Theory (EUT) for evaluating the added resistance of a ship on following waves. In this work, the strip theory was

compared with EUT to compute added resistance of ships. As conclusion of the work, EUT was considered better than strip theory because of the consideration of three dimensional and forward speed effects.

### *1.2.6. Estimating Added Power in Waves for Ships Through Analysis of Operational Data – [6]*

Similarly to this work, this paper has focused on trying to quantify the added power in seaway, from full scale measurement. The calculated approach for estimating the added power due to waves and wind was by deducting the calm water power from the total measured shaft power.

# 2. INVESTIGATION METHOD

The aim of this work is to perform a sensitivity study with respect to the parameters that may have an influence on a ship added power in seaway, by analyzing real data measured on board of a series of six sister container ships of 8400 TEU and approximately 300 m LOA. The measurements related to years 2009 to 2014 while navigating on an Asia - Europe route through Suez Canal. Among other, the recorded data include the following information:

- Date and time of record
- Speed over ground
- Course
- Shaft RPM
- Shaft power
- Geographical Latitude
- Geographical Longitude
- Draft at aft perpendicular
- Draft at forward perpendicular
- Operational Status (departure, arrival, port, anchor stops, EOSP, sea, drifting start)

Based on the date, time, latitude and longitude it is possible to retrieve the environmental conditions the ship faced, such as wave spectra, wind speed, wind direction as well as current speed and direction.

Moreover, the hull lines of the ship were available so that it was possible to calculate the acting forces and moments for the given loading and environmental condition by using DNV GL software called GL Power. To better understand the basic steps taken to perform this analysis a flowchart is shown in Figure 1.

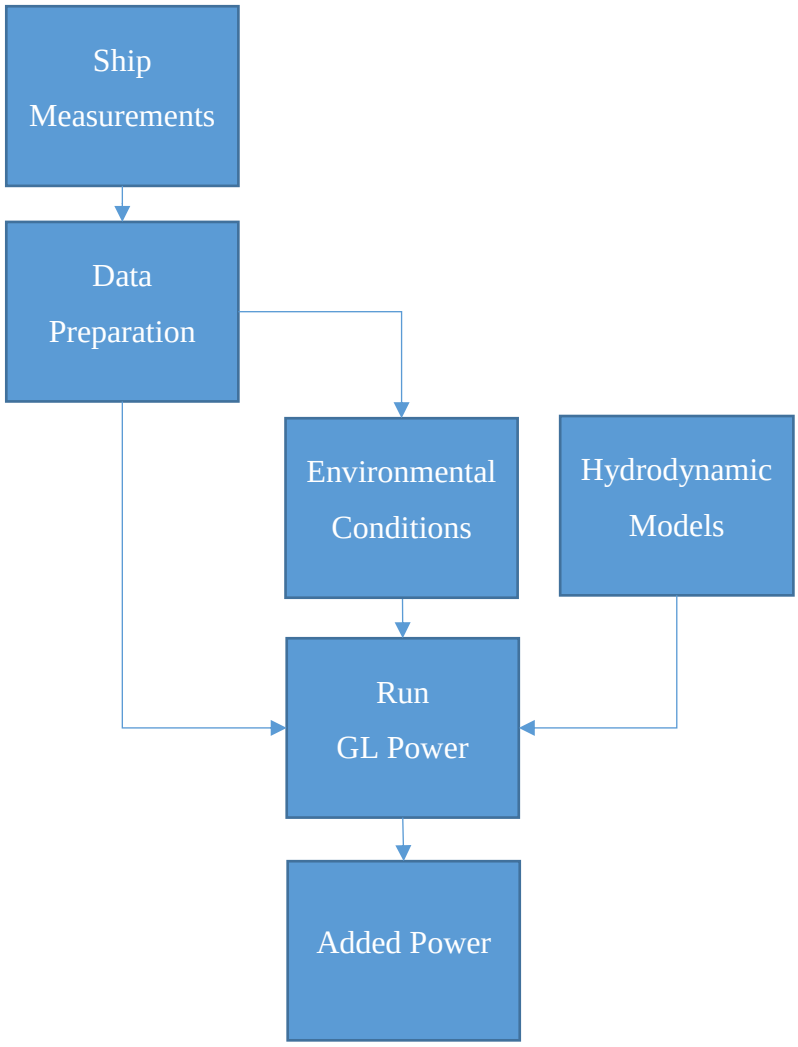


Figure 1 - Schematic of steps taken.

## 2.1. Data preparation

Cleaning the available measurement data had a major importance to begin this study, as the data provided by the shipowner summed altogether almost 295.000 measurements. To avoid inconsistencies, as well as to be sure that the sensitivity study would occur in a proper and controlled range of data the following items were disregarded in the study:

- Shaft RPM < 20 RPM
- Speed over Ground < 10.0 knots
- Trim > 3.5m
- Shaft power < $10^6$ W
- All events where it was stated by the captain that the ship was not on full navigating condition (e.g. Departure, Arrival, PORT, Anchor Stops)

After applying these filters, the number of the remaining conditions was about 170.000 cases, which can be observed on Figure 2.

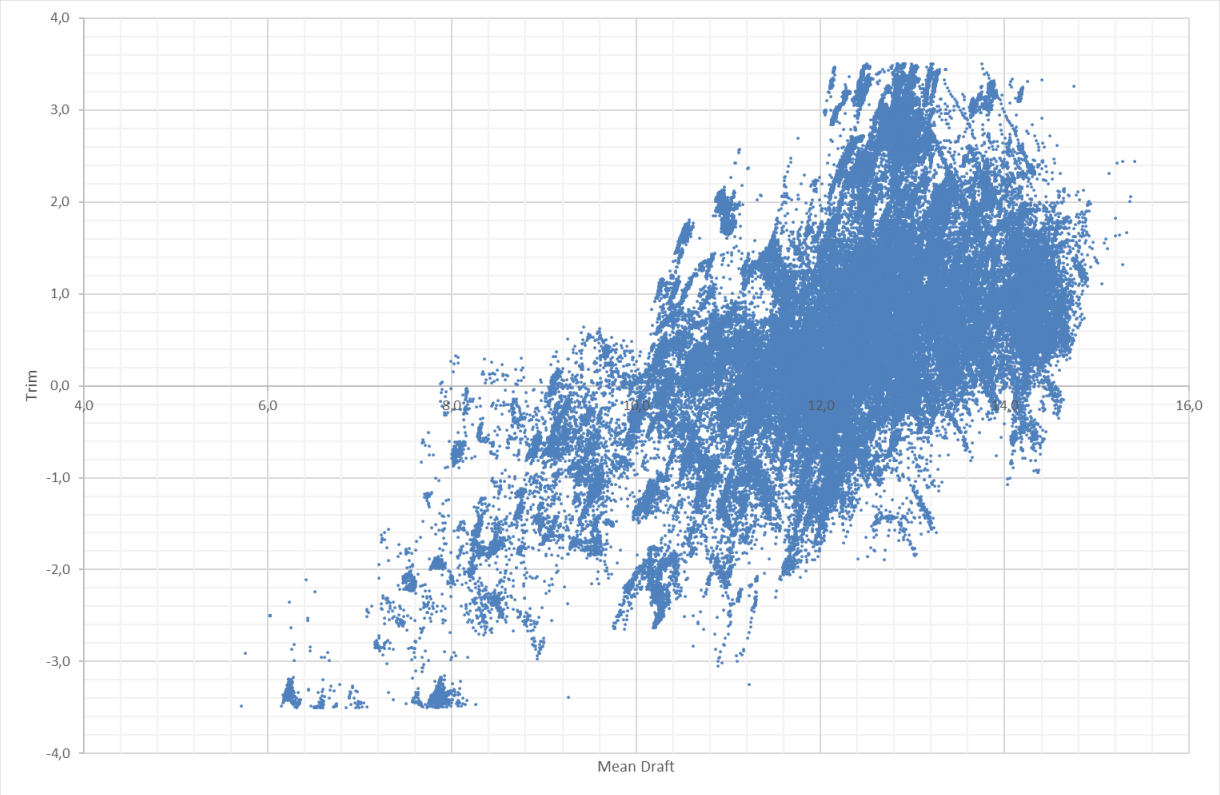


Figure 2 – Filtered loading conditions.

## 2.2. Environmental Conditions

Based on the date, time, latitude and longitude provided by the shipowner, a script was developed to download the environmental conditions from the websites sources [6] and [8] to include those conditions on the previous filtered table provided by the shipowner. This was done to be further possible to run another script by reading this tables lines and running GL Power Software.

The data extracted was wave energy spectra (directions and frequencies as components), current speed, current direction, wind speed and wind direction.

## 2.3. Hydrodynamic Model

Calm-water derivatives, wind force coefficients, open-water propeller characteristics, and wave drift forces for this series of ships were provided by DNV GL as input to this study. Calm-water

derivatives were obtained via CFD – RANSE (computational fluid dynamics - Reynolds-Average Navier-Stokes equations) and model basin tests, where components of x- and y- forces and moment with respect to z direction are given, see Figure 3. Open water propeller characteristics (J - advance ratio, $K_T$ - thrust coefficient and $K_Q$ - torque coefficient). Coefficients of wind force and moments were defined from wind tunnel tests. Wave drift forces were obtained by running a linear 3d Rankine source-patch method GL Rankine, for a given set of loading conditions (drafts, trims) ship forward speeds, wave frequencies and directions.

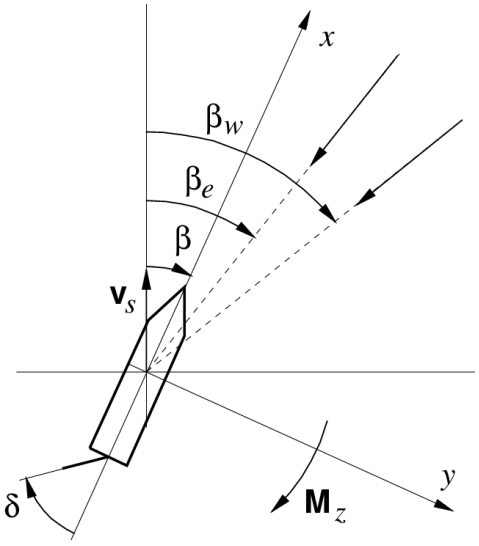


Figure 3 – Coordinate system (picture from GL Power manual).

## 2.4. GL Power Software

GL Power was the software used to calculate the added power of the ship by combining the input information described in items 2.1, 2.2 and 2.3 above. The software solves the equilibrium equation of forces and moments (1) to (3) in coordinate system shown in Figure 3 with the origin O in the intersection of waterplane, central plane and midship transversal plane. X positive pointing towards bow, Y towards starboard and moment around Z downward.

$$X_S + X_W + X_d + X_R + T(1-t) = 0 \quad (1)$$

$$Y_S + Y_W + Y_d + Y_R = 0 \quad (2)$$

$$N_S + N_W + N_d + N_R - Y_R L_{PP}/2 = 0 \quad (3)$$

Here X and Y are force projections on x and y directions, N moments around z axis, T propeller thrust and t is thrust deduction. The subscripts s, w, d and R refer to calm water hydrodynamic reaction, wind load, drift load due to waves and rudder forces, respectively.
One of the various outputs produced by the software is the required delivered power for the given input conditions.
The final output of the work is a comparison of the numerical result with measurements.

## 2.5. Sensitivity Study

The sensitivity study was performed by comparing the measured power of the ship for each given environmental condition against the required delivered power given as output from GL Power. The main goal of the sensitivity study is to evaluate the influence of wind, current and waves on the final added power of the ship in seaway. This and other graphical enabled the author to investigate which parameters have a major influence on the added power of a ship on seaway.
The result of this investigation can serve as input to industry on where to focus the attention when in the prediction of added power in seaway, as well as how to improve route optimization tools.

# 3. POST PROCESSING OF MESUREMENTS

Based on the reported data for each ship, it is possible to retrieve the actual environmental data faced by the ship, by accessing environmental databases available. It would be extremely difficult to accomplish such task manually, as the measurements report had more than 100.000 cases. Thus, a software tool was developed to automatically retrieve wind speed, wave energy spectra and current. These data served as input for GL Power.

## 3.1. Environmental Conditions

Wind and wave information was retrieved from the European Centre for Medium-Range Weather Forecasts (ECMWF) website where a project called ERA-Interim [8] performs a reanalysis of its archived observations using a forecast model and data assimilation systems from 1979 until present days. Public datasets are available for downloading.
Ocean current information were obtained from the Physical Oceanography Distributed Active Archive Center (PO.DAAC) website which is a part of the group Earth Observing System Data and Information System (EOSDIS) that provides science data for NASA's Science Mission Directorate.
PO.DAAC, among many available environmental data, has a project called OSCAR (Ocean Surface Current Analysis Real-time), [6], with the near-surface ocean currents information.

### *3.1.1. Wind Information*

Wind information was retrieved with a script in Python language. The data are available for a grid of 0.75º by 0.75º with measurements steps of 6:00 hours.
The information was downloaded in a Network Common Data Form (NetCDF) file format, where information on latitude, longitude, zonal velocity (positive for west to east wind), meridional velocity (positive for south to north wind) and date and time of measurements are stored.

### *3.1.2. Wave information*

Wave information was retrieved from ERA-Interim as 2D Wave Spectra, where the energy spectra defined at 30 frequencies and 24 directions. Frequencies were distributed geometrically with a 1.1 step, according to Eq. (4), where f(0) = 0.0345 Hz, whereas the directions range

started on 7.5 degrees with a step of 5º for 36 directions. A wave propagating to north is a 0º wave.

$$f(n) = f(n-1) \cdot 1.1 \tag{4}$$

The energy spectrum data are encoded as a logarithm of base 10, thus the wave energy spectra should be 10 to the power of the value provided.
The wave input information was downloaded for the same grid of locations, date and time and in the same file format (NetCDF).

#### *3.1.3. Ocean Current*

The ocean current information was obtained from the OSCAR project [7], where it is available since October 5th,1992 at the frequency of 172 per scan, i.e. approximately every 5 days, on a spatial grid of 1/3º in latitude and longitude directions. The measurements considered a near-surface ocean current with an average depth of 15 m below water level.
The file format used to download this information was also NetCDF, containing information about latitude, longitude, date and time similarly to the above described.

## 3.2. Resulting Database

A script written on Python was developed to read each line of the shipowner database and include the measured environmental conditions as additional columns in the original spreadsheet.
Because, the spatial and temporal grids vary from file to file and don't match with the latitude, longitude, date and time of the measurements, interpolated values were used (5).

$$\begin{aligned} \mathrm{u} = \hat{h}\hat{l}\hat{d}\big(&u_{d2,l2,h2} - u_{d1,l2,h2} - u_{d2,l1,h2} + u_{d1,l1,h2} - u_{d2,l2,h1} + u_{d1,l2,h1} \\ &+ u_{d2,l1,h1} - u_{d1,l1,h1}\big) \\ &+ \hat{l}\hat{h}\big(u_{d1,l2,h2} - u_{d1,l1,h2} - u_{d1,l2,h1} + u_{d1,l1,h1}\big) \\ &+ \hat{h}\hat{d}\big(u_{d2,l1,h2} - u_{d1,l1,h2} - u_{d2,l1,h1} + u_{d1,l1,h1}\big) \\ &+ \hat{l}\hat{d}\big(u_{d2,l2,h1} - u_{d1,l2,h1} - u_{d2,l1,h1} + u_{d1,l1,h1}\big) \\ &+ \hat{l}\big(u_{d2,l2,h1} - u_{d1,l1,h1}\big) + \hat{d}\big(u_{d2,l1,h1} - u_{d1,l1,h1}\big) \\ &+ \hat{h}\big(u_{d1,l1,h2} - u_{d1,l1,h1}\big) + u_{d1,l1,h1} \end{aligned} \tag{5}$$

Where:

$$\hat{d} = \frac{d-d1}{d2-d1}, \hat{l} = \frac{l-l1}{l2-l1}, \hat{h} = \frac{h-h1}{h2-h1} \quad (6)$$

and d=time, l= longitude, h=latitude; 1=left boundary, 2= right boundary and d, l and h without index is the point of interest.

## 3.3. Environmental Data Consistency Check

To verify consistency of environmental data, a random check was performed comparison with some website sources which use the same database as the ones referred in this thesis, (e.g. LAS – Live Access Server, http://thredds.jpl.nasa.gov/las/ ).

All consistency checks performed gave confidence that script developed was running well without numerical inconsistencies.

# 4. ADDED POWER CALCULATION

In this section there will be a brief discussion on how to run the software GL Power, the equations it is solving, input and output file examples as well as the method to obtain the calculated added power of the ship in given conditions.

## 4.1. GL Power Input Files

The aim of this section is to briefly discuss the input files and method of solution used by this software.

Figure 4 illustrate an example of input file for GL Power.

```
old 8400 TEU, draft 13.24 m
317.2     331.17     13.24                              # Lpp, Loa, Tm
1796.8    10397.8                                       # Afr, Alt
8.5       0.26       0.16   5.71e7    1.733   0.0    10.0  # Dpr, wft, thdf, MCR, nprop0,cMCR,vMCR
70.32     61.136     6.582  7.325     12.450  7.193        # Arud, Arp, xdrud, crud, erud, chmr
1025.0    1.20                                          # rhw, rha
2.9366e-2 4.5467e-3  0.0    2.5550e-4                     # CArud, CDrud0, CBrud, CCrud
old8400cw10.803.dat                                     # Drift forces in calm water
old8400wind.dat                                         # Wind forces
old8400wave.dat                                         # Wave dirf forces
old8400prop.dat                                         # Propeller Curves
Spc-14-Feb-01_Time_00-05-Ln-118.90-Lt-19.41.csv          # Wave Spectra
164.13 10.57 1.69 8.76                                  # wind direction, deg., wind speed, m/s, sign. wave height, m, Ship Speed, m/s
```

Figure 4 - GL Power input example.

### *4.1.1. Calm-Water Reactions*

Coefficients of calm-water reactions are provided in an input file that has a structure of four columns, containing the drift angle β[°], the non-dimensional coefficients $X'_S(\beta)$ , $Y'_S(\beta)$ and $N'_s$ as shown in Figure 5.

```
  0.0 -8.47255E-3 0.0          0.0
  5.0 -8.47255E-3 1.01720E-2   1.06570E-2
 10.0 -8.23074E-3 3.06250E-2   2.83650E-2
 15.0 -6.91618E-3 6.23590E-2   4.64890E-2
 20.0 -3.74908E-3 1.00000E-1   5.87500E-2
 25.0 -4.99878E-4 1.40000E-1   6.24170E-2
 30.0  2.96402E-3 1.88150E-1   6.45300E-2
 35.0  6.24847E-3 2.40000E-1   6.60000E-2
 40.0  6.24847E-3 2.97000E-1   6.68250E-2
 45.0 -1.90260E-2 3.53618E-1   6.61136E-2
 60.0 -1.82607E-2 5.72256E-1   6.10393E-2
 75.0 -9.51600E-3 7.33430E-1   4.95574E-2
 90.0 -6.87998E-3 7.83069E-1   2.97039E-2
105.0 -1.02967E-2 7.48509E-1 -7.05800E-4
120.0 -1.00708E-4 6.13138E-1 -1.97187E-2
135.0 -5.43539E-4 4.28259E-1 -3.28799E-2
150.0 -1.87879E-2 2.92472E-1 -4.71171E-2
165.0 -4.59016E-3 1.89111E-1 -2.85644E-2
180.0  5.89639E-3 0.0          0.0
```

Figure 5 - Calm-water coefficients input file.

Those non-dimensional derivatives are used to calculate de calm water forces as per. (7) to (9).

$$X_S = X'_S(\beta)\frac{\rho}{2}{v_s}^2 L_{pp} T_m \tag{7}$$

$$Y_S = Y'_S(\beta)\frac{\rho}{2}{v_s}^2 L_{pp} T_m \tag{8}$$

$$N_S = N'_S(\beta)\frac{\rho}{2}{v_s}^2 {L_{pp}}^2 T_m \tag{9}$$

where, $\rho$ is water density, $v_s$ is ship speed, $L_{pp}$ length between perpendiculars and $T_m$ draft midship.

The calm water derivatives input files used to perform this study were for the drafts of 13,0m and 13,5m. Those files were obtained from model test combined with CFD-RANSE simulations, which as can be seen from the histogram below is a representative range of the represented loading conditions reported.

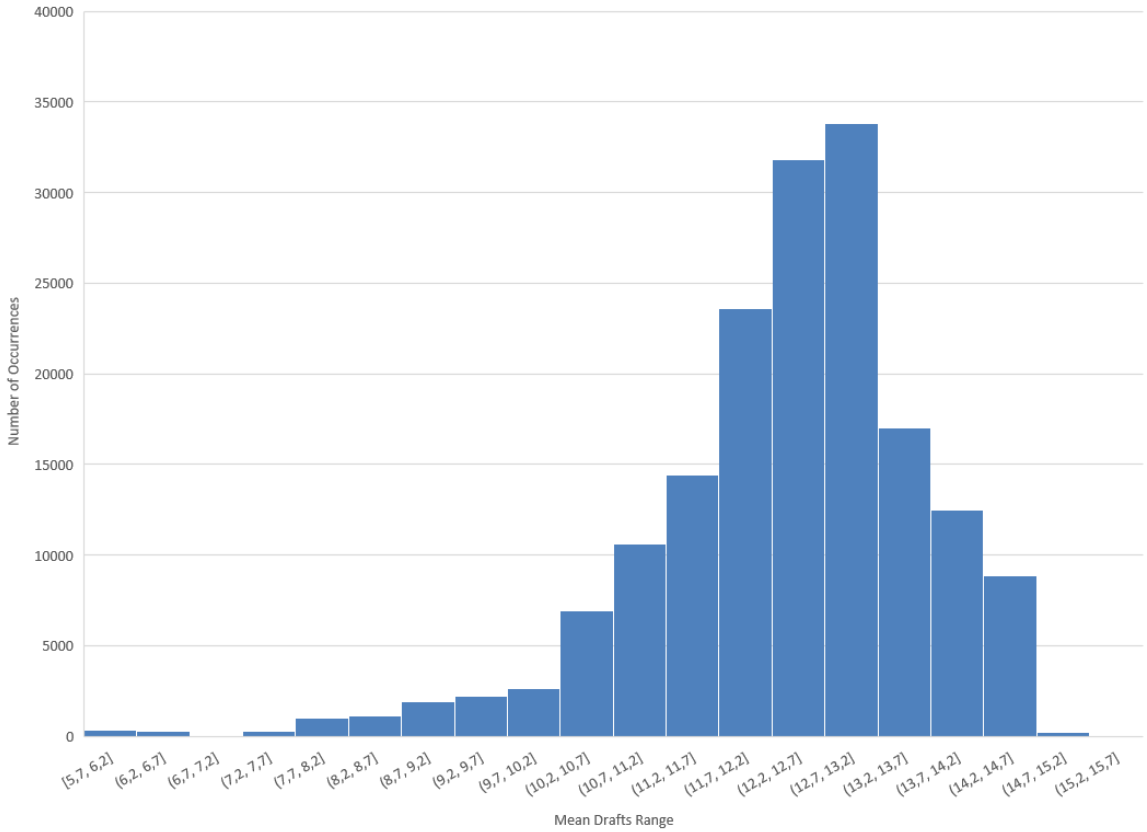


Figure 6 - Histogram with mean draft.

### *4.1.2. Wind Force*

Wind force and moments are calculated from the wind forces as shown in eqs. (10) to (12).

$$X_w = X'_w(\varepsilon)\frac{\rho_a}{2}{v_w}^2 A_F \tag{10}$$

$$Y_w = Y'_w(\varepsilon)\frac{\rho_a}{2}{v_w}^2 A_L \tag{11}$$

$$N_w = N'_w(\varepsilon)\frac{\rho_a}{2}{v_w}^2 A_L L_{oa} \tag{12}$$

Where, $\rho_a$ is air density, $v_w$ apparent wind speed, $A_F$ forward projected area above waterline and $A_L$ lateral projected area above waterline. The input file has a similar structure as calm-water reactions consisting of four columns, being the first column the apparent wind angle of attack $\varepsilon$ [º] and second, third and fourth column with aerodynamical coefficients $X'_w(\varepsilon)$, $Y'_w(\varepsilon)$ and $N'_w(\varepsilon)$.

### *4.1.3. Wave Drift Forces*

Wave drift forces are calculated in GL Power using the spectral method (13).

$$\overrightarrow{F_d} = 2\int_0^\infty\int_0^{2\pi}\frac{\overrightarrow{F_d}(u_s,\mu,\omega)}{{\zeta_a}^2}S_{\zeta\zeta}(\omega)D(\mu)d\omega d\mu \tag{13}$$

$\overrightarrow{F_d}/{\zeta_a}^2$ is the quadratic transfer function of the mean longitudinal and lateral drift forces and yaw moments $u_s$ longitudinal ship speed, $\mu$ is the mean wave direction, $\zeta_a$ is the wave amplitude, $S_{\zeta\zeta}$ is the wave spectrum and D is the spreading function.

From GL Rankine transfer functions results are input file to GL Power. The input file has six columns being the first column the forward speeds [m/s], second column wave frequencies [rad/s], third column wave directions [º], fourth column x-drift forces per wave amplitude squared [kN/m²], fifth column y-drift forces per wave amplitude squared and last column z-drift moment per wave amplitude squared [kN.m/m²]. An example of input file is show on Figure 7.

```
13.118  0.18    0.0     11204.25959748921       -0.8361117179021775     -246.5514059089783
13.118  0.2     0.0     10941.446221841166      -0.22409874740659752    -160.81355169634188
13.118  0.22    0.0     11024.45797864047       -2.0123150020648213     -99.51583768231626
13.118  0.24    0.0     11440.479183294123      -2.0286435071677835     -84.70852693050739
13.118  0.26    0.0     12005.022792282562      -1.9274754981971831     -172.4649030647876
13.118  0.28    0.0     12296.54133483995       -0.957398659209971      -155.0933497178152
```

Figure 7 – Wave drift forces input.

This input file would ideally have to be generated for all cases of study. However, this would lead to an enormous computational time. Thus, it was decided to limit the number of cases to run in GL Rankine to an envelope of the reported loading conditions. In this way, to determine the wave-drift forces for each loading condition, the input file was generated by interpolating the envelope surrounding cases or considering the nearest case if the loading case was outside the envelope region. The calculated envelope conditions are shown on Figure 8.

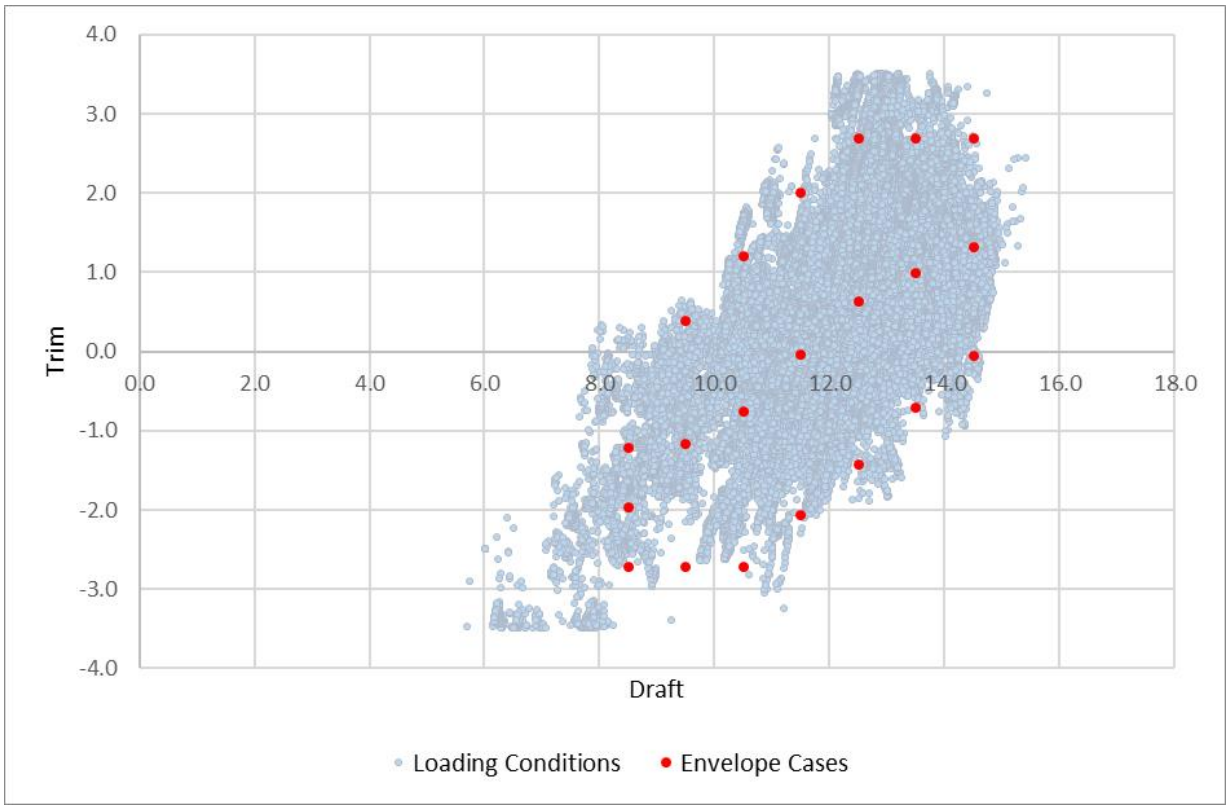


Figure 8 - Wave drift forces envelope conditions.

### *4.1.4. Propeller Characteristics*

The propeller thrust and torque are obtained from the input of open-water propeller characteristics. The file contains three columns being the first column the advance ratio J, second column thrust coefficient $K_T(J)$, and third column torque coefficient.

### *4.1.5. Rudder Forces*

The forces in x and y directions on the rudder are calculated as per eqs. (14) and (15) respectively, while the equations of moment around z is shown in eq. (16).

$$X_R = -L\sin(\alpha - \delta) - D\cos(\alpha - \delta) \tag{14}$$

$$Y_R = L\cos(\alpha - \delta) - D\sin(\alpha - \delta) \tag{15}$$

$$N_R = -Y_R l_R \tag{16}$$

L is lift force, D is drag force, $\delta$ rudder angle and $\alpha$ is the angle of attack of rudder with respect to surrounding flow. Lift and drag forces can be determined from eqs. (17) and (18).

$$\mathrm{L} = C_L(\alpha)\frac{\rho}{2}{v_R}^2 A_R \tag{17}$$

$$\mathrm{D} = C_D(\alpha)\frac{\rho}{2}{v_R}^2 A_R \tag{18}$$

$C_D(\alpha)$ is rudder drag coefficient, $C_L(\alpha)$ is rudder lift coefficient, $v_R$ is the average flow speed around the rudder, $A_R$ is the rudder submerged projected area and $\rho$ is water density.

### *4.1.6. GL Power Solution Method*

GL Power iteratively solves the equations (1) to (3) using equations given on sub-items 4.1.1 to 4.1.5, resulting on a non-linear system shown in eqs. (19) to (21). Thus, this non-linear system can be solved with respect to T, $\alpha$ and $\beta$.

$$\begin{aligned} T + X'_w(\varepsilon)\frac{\rho_a}{2}{v_w}^2 A_F + X'_S(\beta)\frac{\rho}{2}{v_s}^2 L_{pp} T_m + X_d(\mu, u) - C_L(\alpha)\frac{\rho}{2}{v_R}^2 A_R \\ - C_D(\alpha)\frac{\rho}{2}{v_R}^2 A_R = 0 \end{aligned} \tag{19}$$

$$\begin{aligned} Y'_S(\beta)\frac{\rho}{2}{v_s}^2 L_{pp} T_m + Y'_w(\varepsilon)\frac{\rho_a}{2}{v_w}^2 A_L + Y_d(\mu, u) + C_L(\alpha)\frac{\rho}{2}{v_R}^2 A_R \\ - C_D(\alpha)\frac{\rho}{2}{v_R}^2 A_R = 0 \end{aligned} \tag{20}$$

$$\begin{aligned} C_L(\alpha) l_R \frac{\rho}{2}{v_R}^2 A_R - N'_w(\varepsilon)\frac{\rho_a}{2}{v_w}^2 A_L L_{oa} + N'_S(\beta)\frac{\rho}{2}{v_s}^2 {L_{pp}}^2 T_m - N_d(\mu, u) \\ - C_D(\alpha) l_R \frac{\rho}{2}{v_R}^2 A_R = 0 \end{aligned} \tag{21}$$

From the result of thrust force T, it is possible to calculate J using eq.(22).

$$\mathrm{T} = \frac{\rho {u_a}^2 D_p K_T(J)}{J^2} \tag{22}$$

Propeller rotation can be found from eq.(23).

$$\mathrm{n} = \frac{u_a}{J D_p} \tag{23}$$

The required delivered power can be obtained by (24),

$$P_d = 2\pi\rho n K_Q(J) \tag{24}$$

## 4.2. Ship Added Power Estimation

The strategy to study the added power factors influence on the ship total power was to run GL Power software setting the values of environmental conditions to real conditions and further evaluating the result for the same load case when this specific environmental condition is neglected. From the input file, as shown on Figure 4, the wind speed, wave height and ship speed are numeric inputs. Thus, to neglect wind speed, this value was set to zero, when the wave influence was neglected, wave eight was set to zero, finally when the ocean current was taken in account the ship speed was set to relative ship speed, and to speed over ground value when current was neglected.

Table 1 - Studied cases.

| Case | Wind | Wave | Current |
|---|---|---|---|
| **Case 1** | Neglected | Neglected | Neglected |
| **Case 2** | Considered | Neglected | Neglected |
| **Case 3** | Neglected | Considered | Neglected |
| **Case 4** | Neglected | Neglected | Considered |
| **Case 5** | Considered | Considered | Neglected |
| **Case 6** | Considered | Neglected | Considered |
| **Case 7** | Neglected | Considered | Considered |
| **Case 8** | Considered | Considered | Considered |

The influence of only those parameters were chosen to be first studied due to the simplicity of running the cases on by changing the input files.

By definition, the added power is obtained by deducting calm water power from the total power as described on eq. (25).

$$A_{Power} = P_{Tolal} - P_{Calm} \tag{25}$$

Hence, in this work, the added power was assessed by comparing the total power, against the total power deducted by the cases shown on Table 1.

## 4.3. Added Power Script Development

A second script was developed to analyse and run the software GL Power based on all data provided by shipowner and postprocessed including environmental conditions.
The software was written using Python language, where it went through line by line of the post processed data, and ran GL Power for all cases described in Table 1. After running all cases, the values of delivered power calculated were included in the same post-processed table.

# 5. RESULTS AND ANALYSIS

## 5.1. Added Power

As mentioned in 4.2, the initial approach taken to evaluate the added power was to subtract the calm water power to obtain the added power. However, as expected and shown in [6] results, it is hard to graphically assess the contribution of the added power.

Initially, the comparison made was on the added power measured, which represented the total power measured less the theoretical calm water power obtained from GL Power, against the added power obtained from GL Power software.

Figure 15 to Figure 14 illustrates the results obtained if we deduct the calm water from the total power. This cloudy tendency, agrees with [6] obtained results.

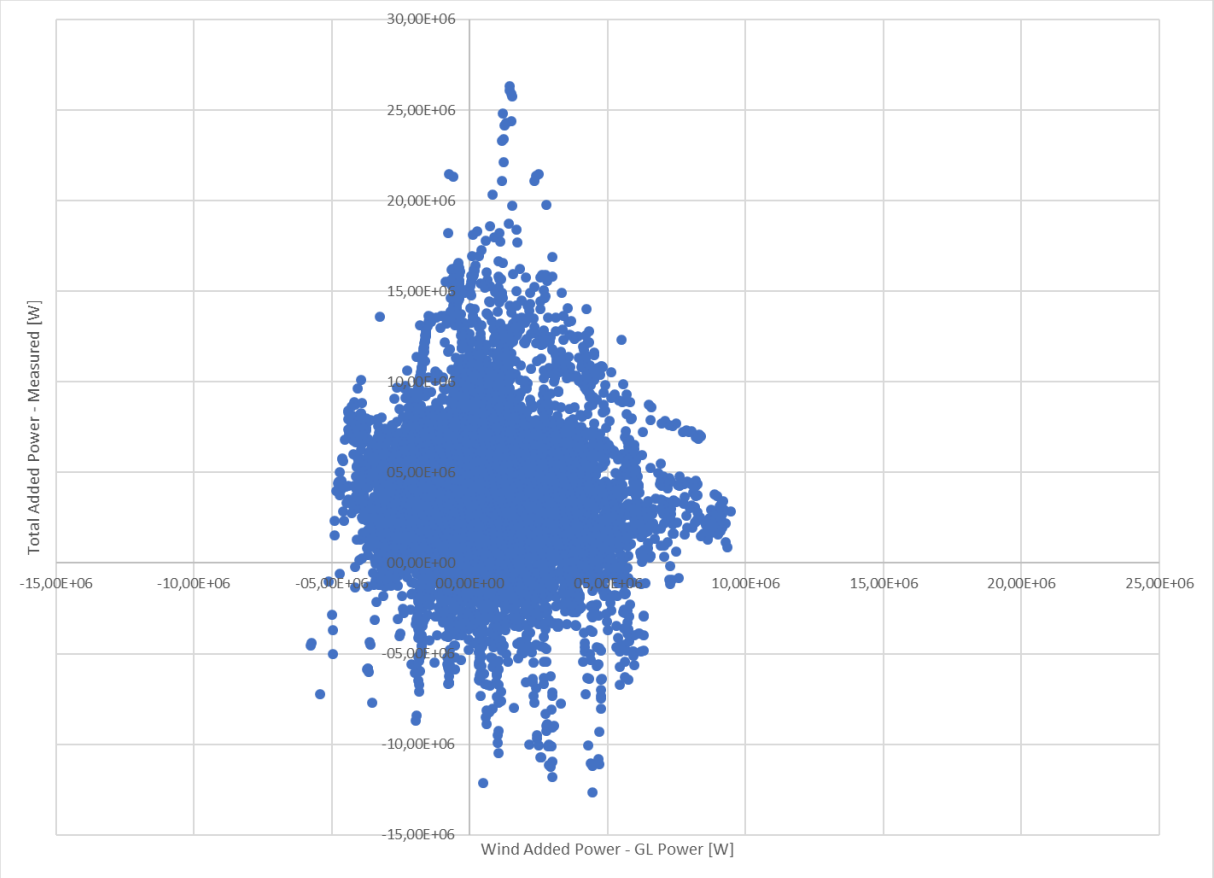


Figure 9 - Total added power due to wind (x-axis) vs. measured (y-axis) – Case 2.

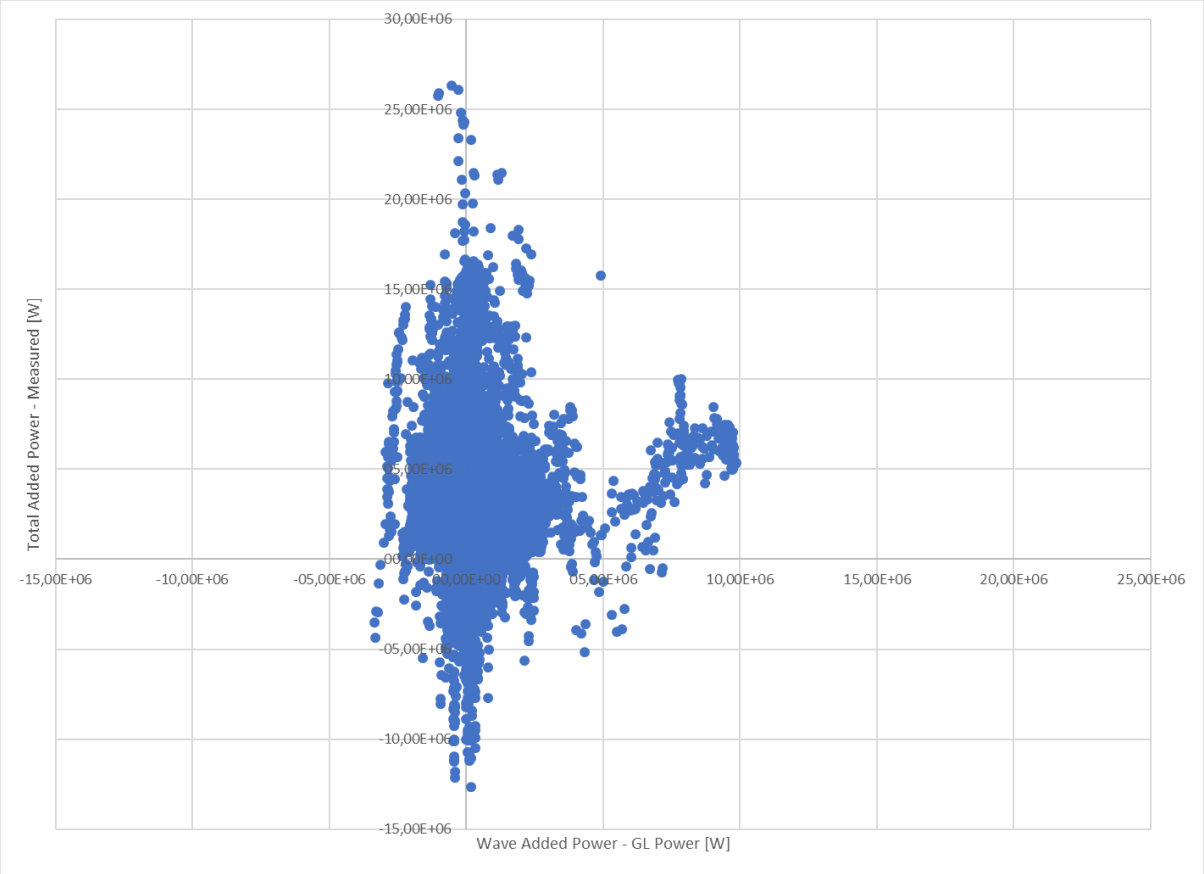


Figure 10 - Total added power due to wave (x-axis) vs. measured (y-axis) – Case 3.

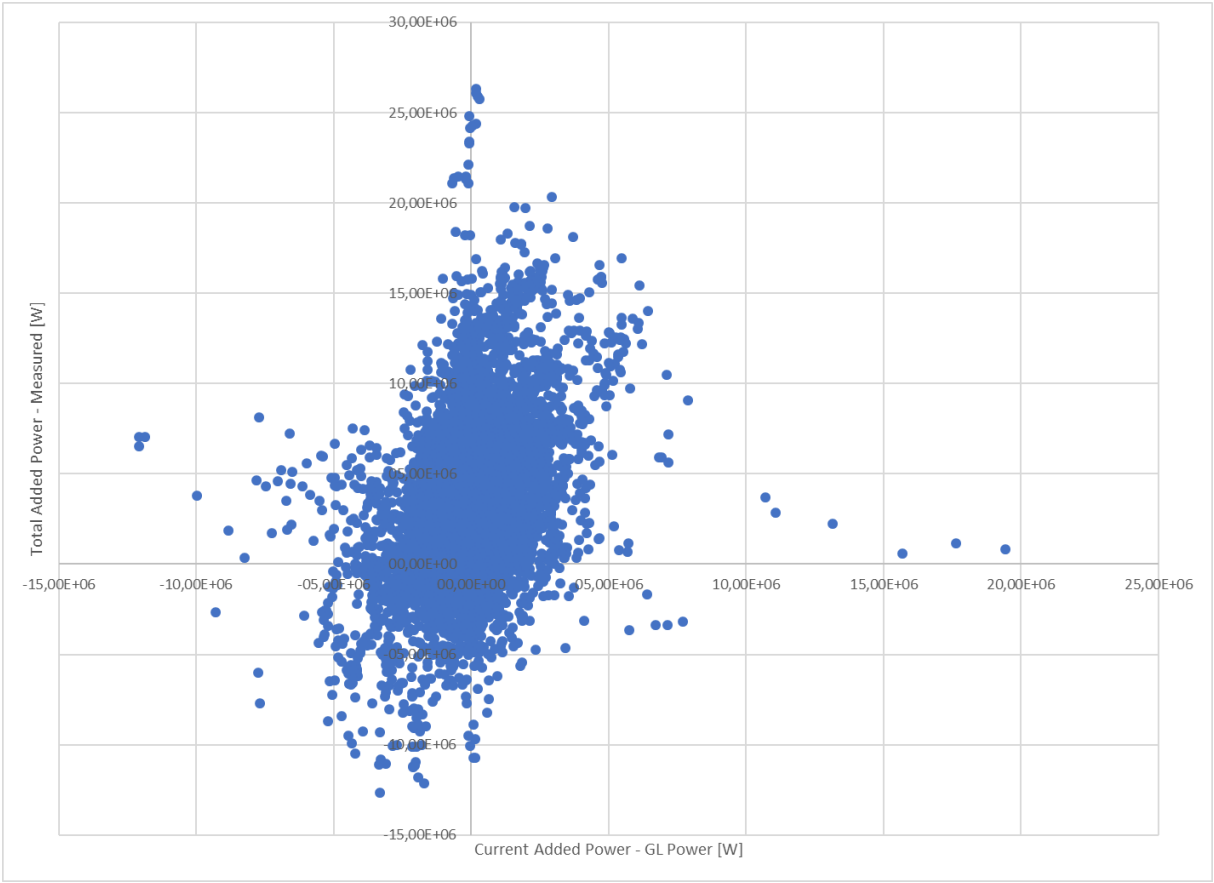


Figure 11 - Total added power due to current (x-axis) vs. measured (y-axis) – Case 4.

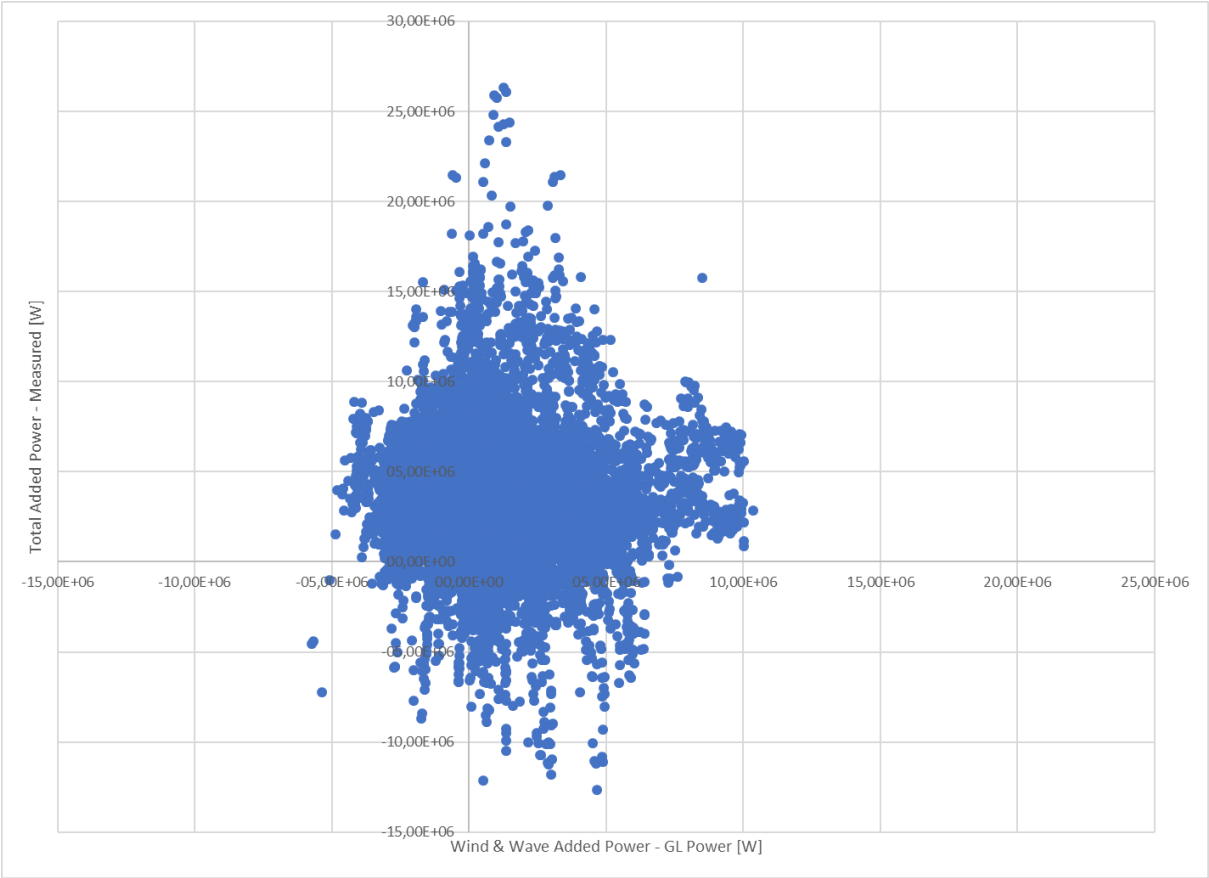


Figure 12 - Total added power due to wind & wave (x-axis) vs. measured (y-axis) – Case 5.

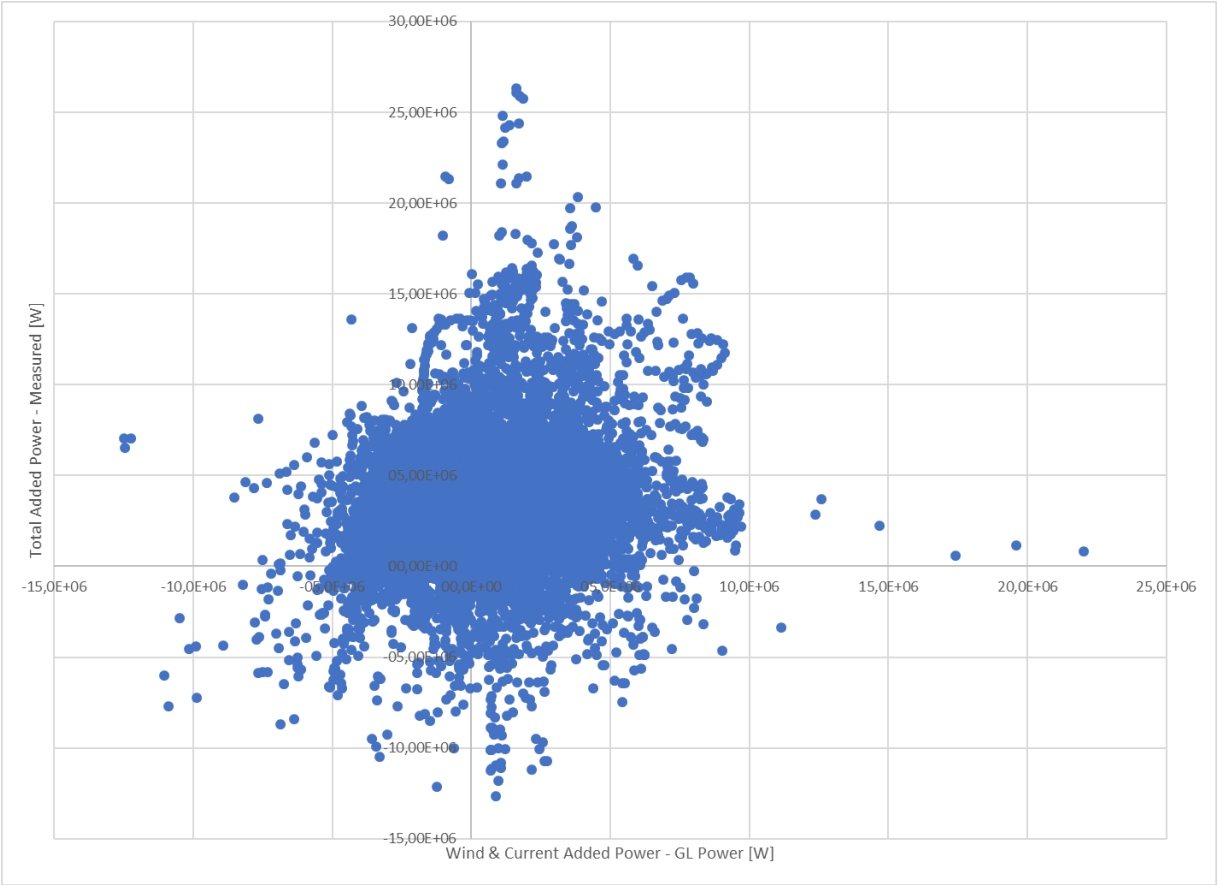


Figure 13 - Total added power due to wind & current (x-axis) vs. measured (y-axis) – Case 6.

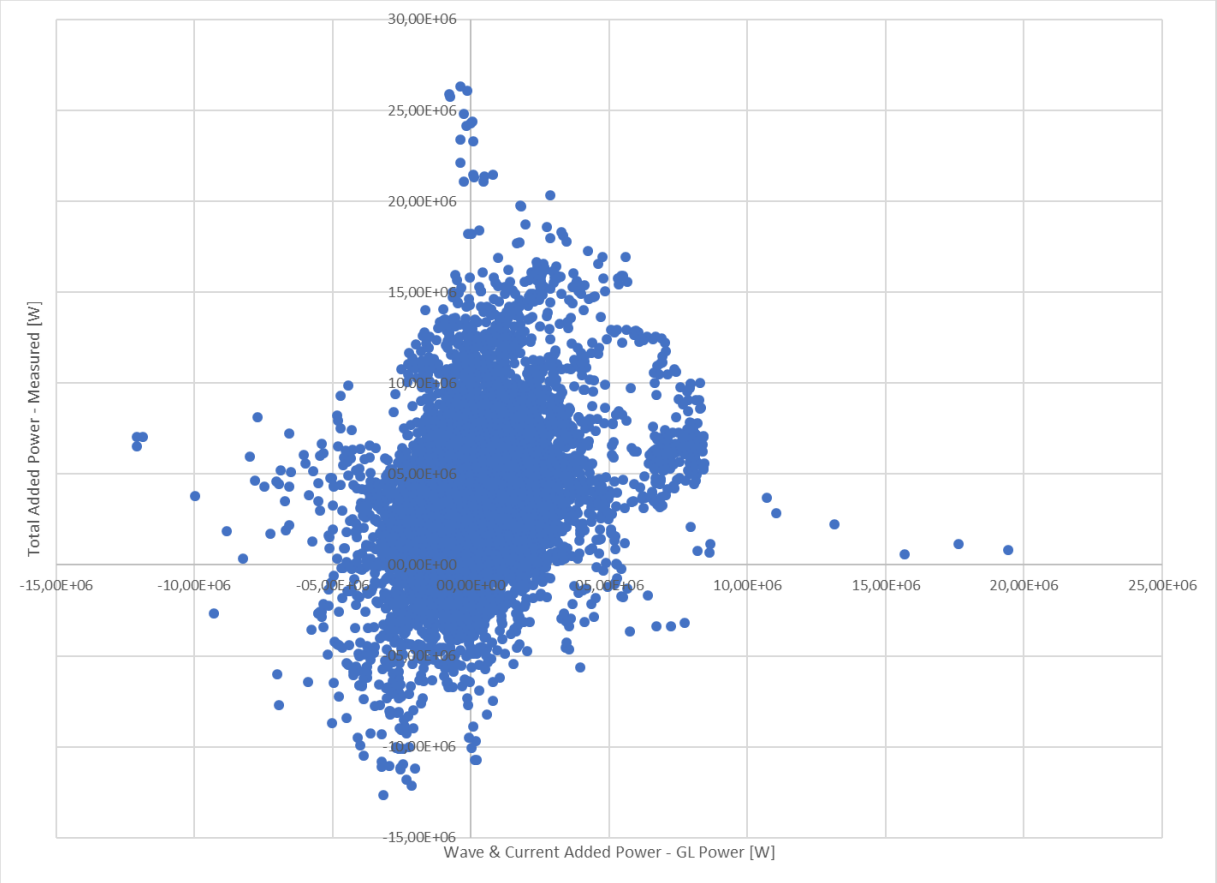


Figure 14 - Total added power due to wave & current (x-axis) vs. measured (y-axis) – Case 7.

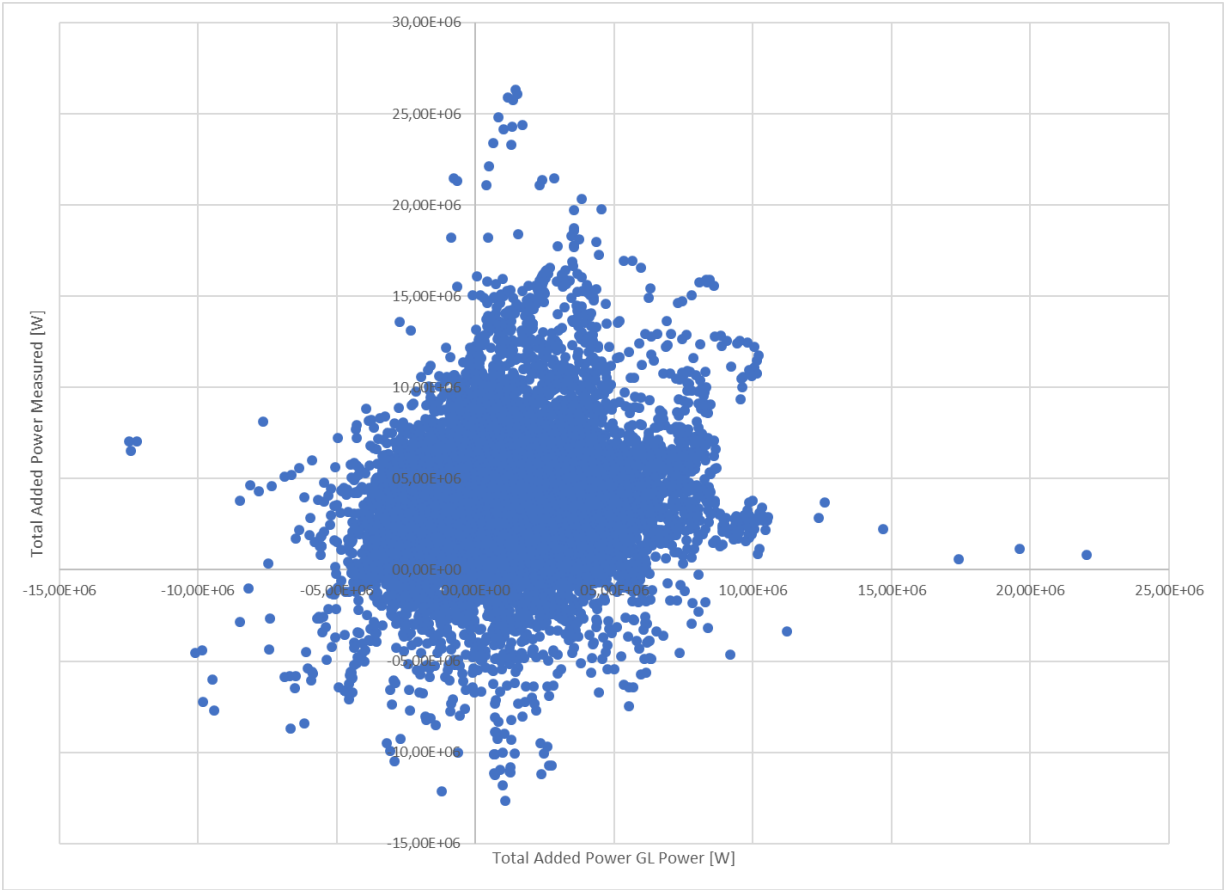


Figure 15 - Total added power computed (x-axis) vs. measured (y-axis) – Case 8.

From Figure 9 to Figure 15 above, it is possible to make a rough qualitative analysis on the influence of the environmental parameters on the final added power. The closer the scatter gets to the y- axis would mean that parameter studied has a minor influence on the final added power, since the calculated value would be closer to zero.

From this rough qualitative analysis, it is possible to see that wind and wave has a major influence on the added power since their clouds are wider.

## 5.2. Total Power

Analysis in the previous section didn't provide a good outlook to evaluate the results. Thus, it was decided to compare the influencing parameters on added power without deducting calm water results.

Initially it was decided to compare the total power measured against the total power calculated. Ideally, this graph should be a perfect fit. The linear regression tool from Microsoft Excel was considered to evaluate the graph tendency and it R-squared values, to check how close the measures are to the fit.

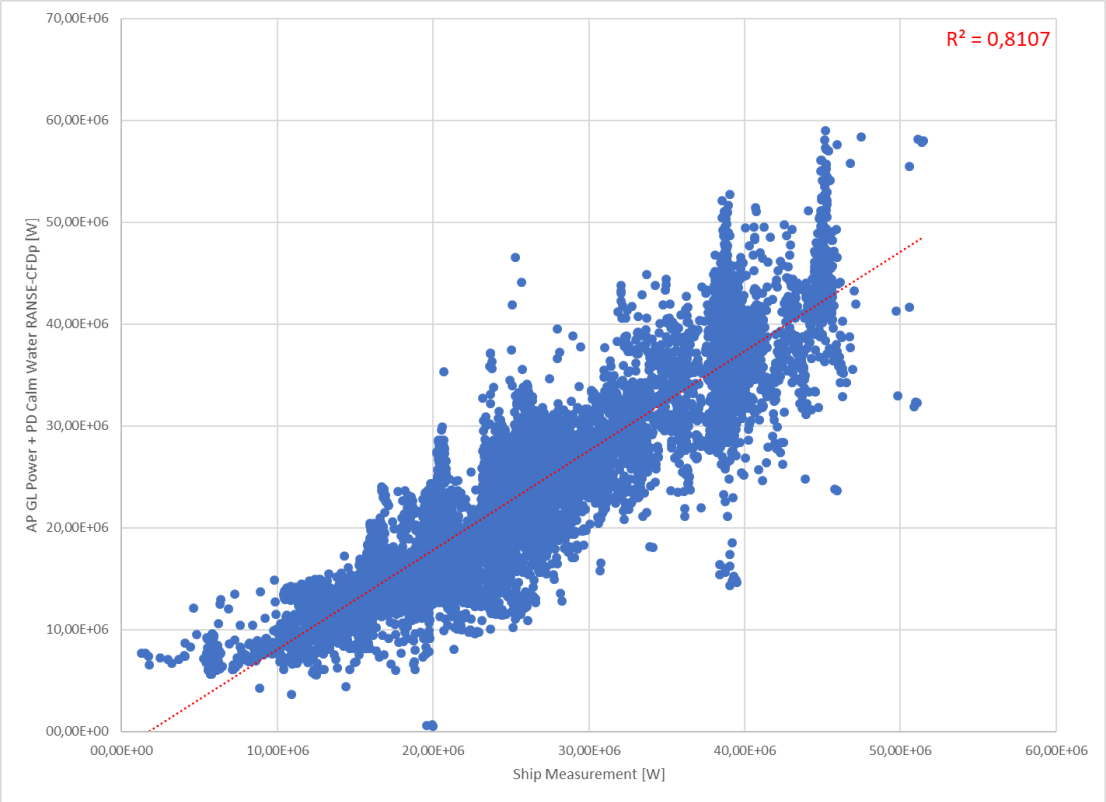


Figure 16 – Total power computed (y-axis) vs. measured (x-axis) – Case 8.

However, as it can be seen from Figure 16, the fit is not passing through origin. Since the ideal correlation should be a linear function passing from origin with slope 1,0, it was decided to evaluate the slope shift from this ideal fit. Using the least squares method, it was calculated the slope of $\theta$ (27) of the new fit that necessarily would cross origin.

$$\theta = \frac{\sum_{i=1}^{N} y_i x_i}{\sum_{i=1}^{N} {x_i}^2} \tag{26}$$

For the case shown in Figure 16, the calculated slope A = 0,915 which can be considered that the proposed method in this work captured about 100% of the added power effect when compared to the measured results.

Before performing an analysis of the calculated added power results against measurements, it was decided to first investigate the influence of the wind, wave and current parameters using numerical results. The comparisons were total calculated power against the calculated power for the cases shown on Figure 18 to Figure 23.

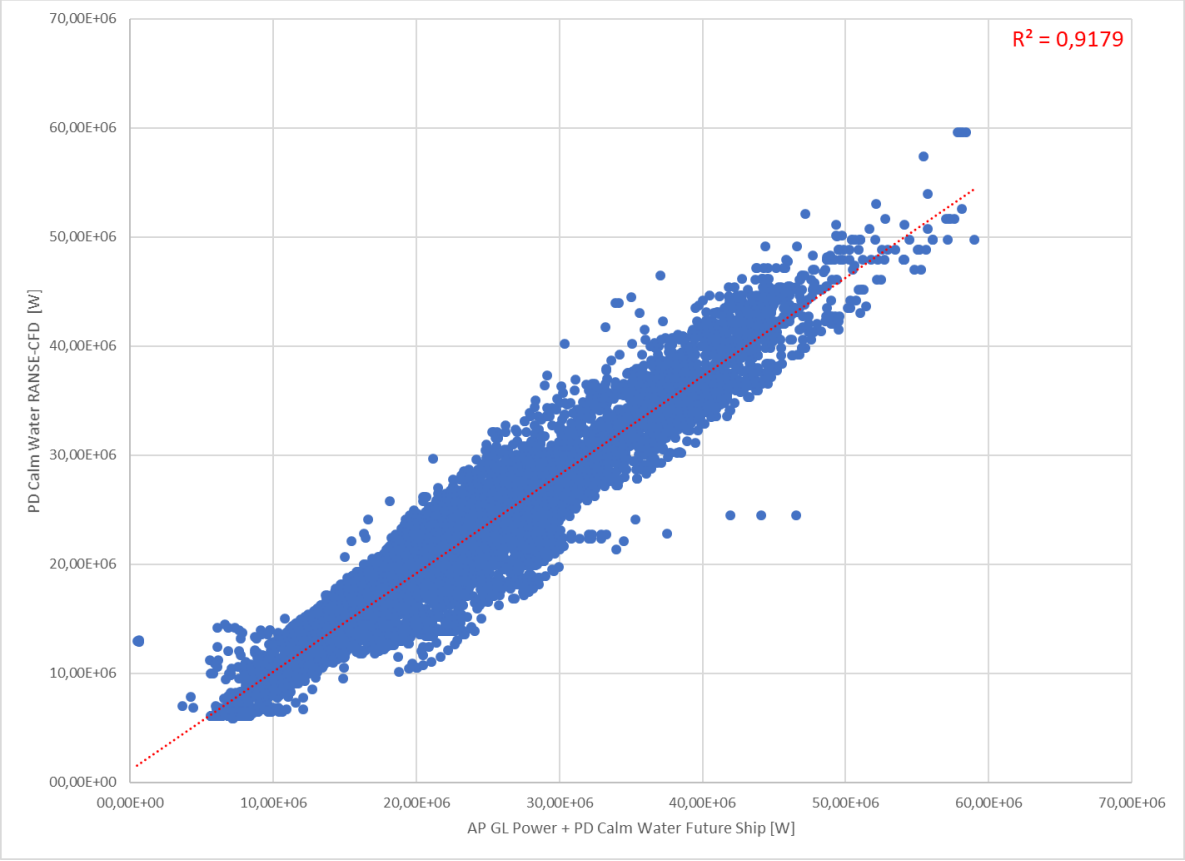


Figure 17 – Theoretical comparison of calm water power (Case 1, y-axis) vs. total calculated power.

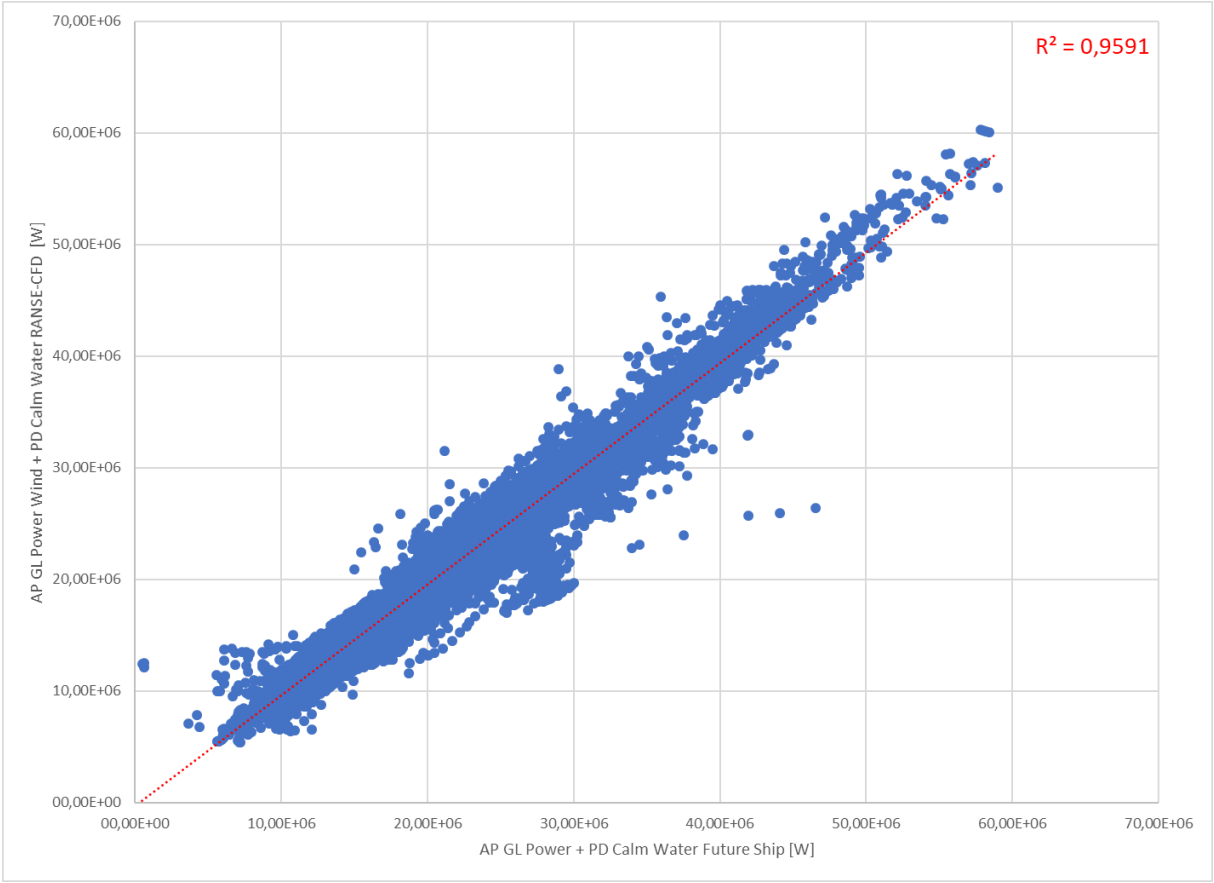


Figure 18 – Theoretical comparison of wind power (Case 2, y-axis) vs. total calculated power.

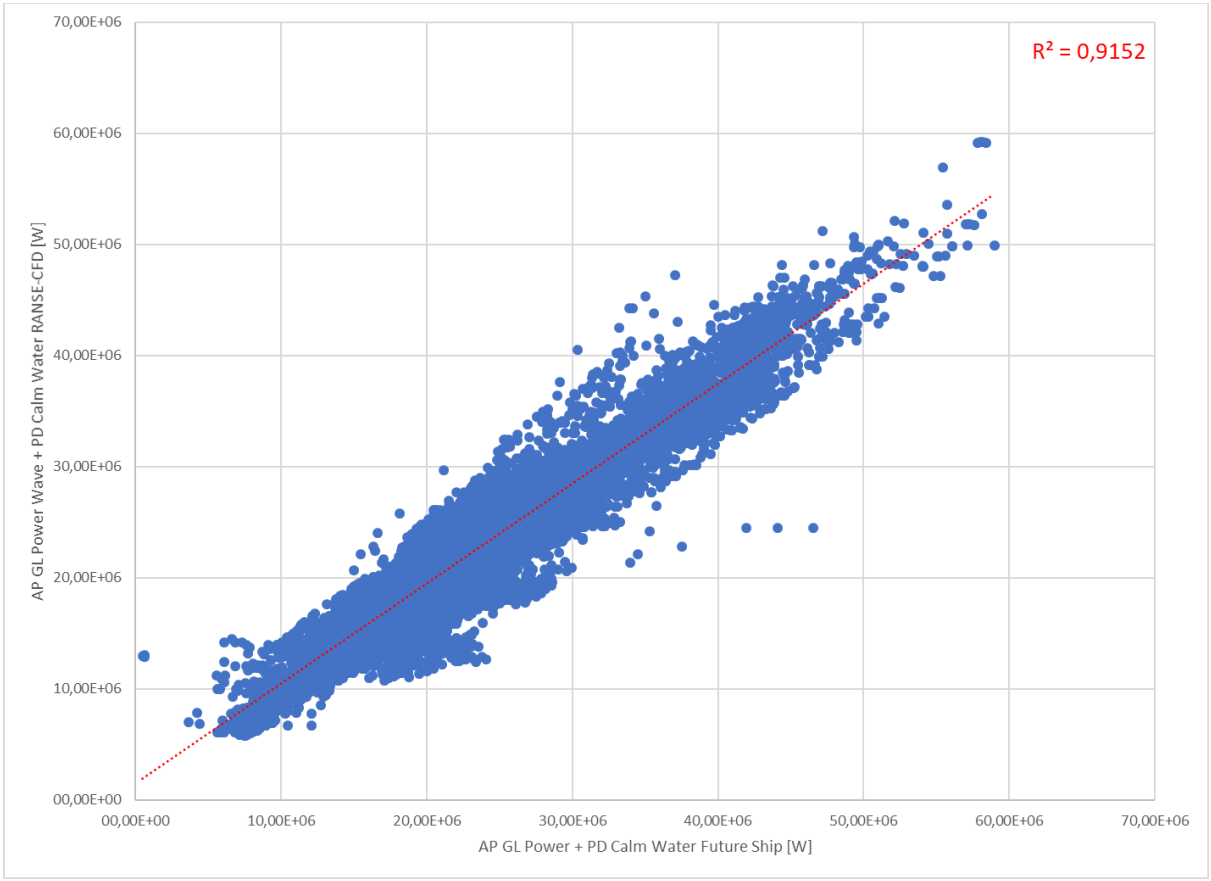


Figure 19 – Theoretical comparison of wave power (Case 3, y-axis) vs. total calculated power.

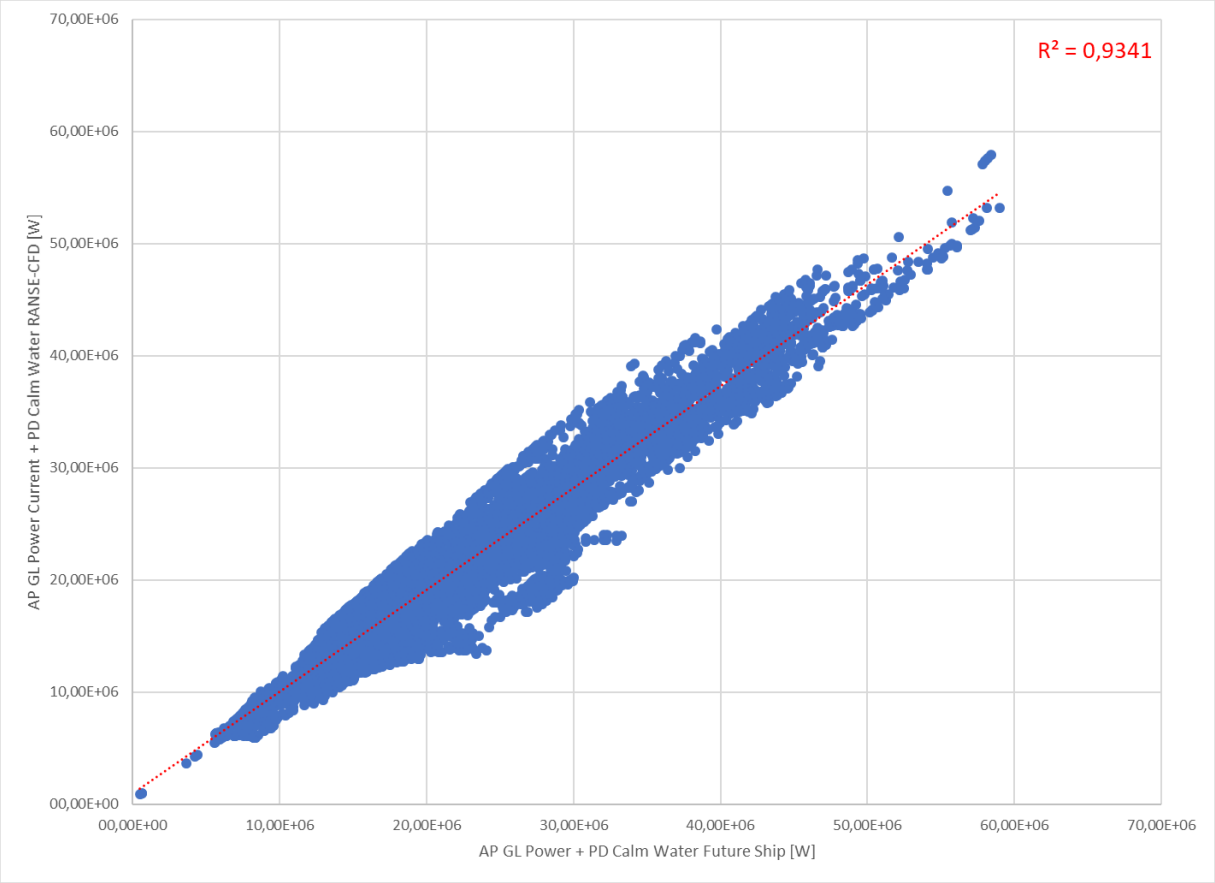


Figure 20 – Theoretical comparison of current power (Case 4, y-axis) vs. total calculated power.

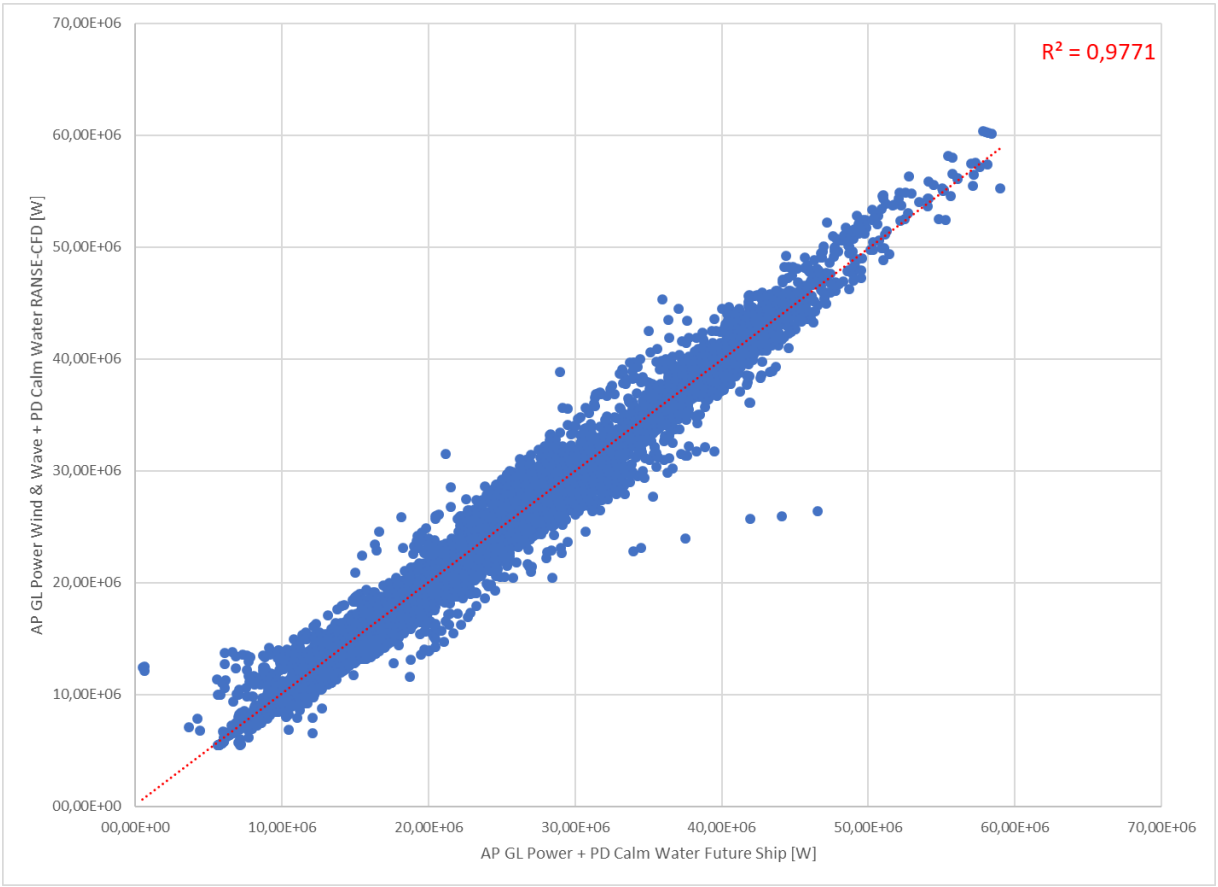


Figure 21 – Theoretical comparison of wind & wave power (Case 5, y-axis) vs. total calculated power.

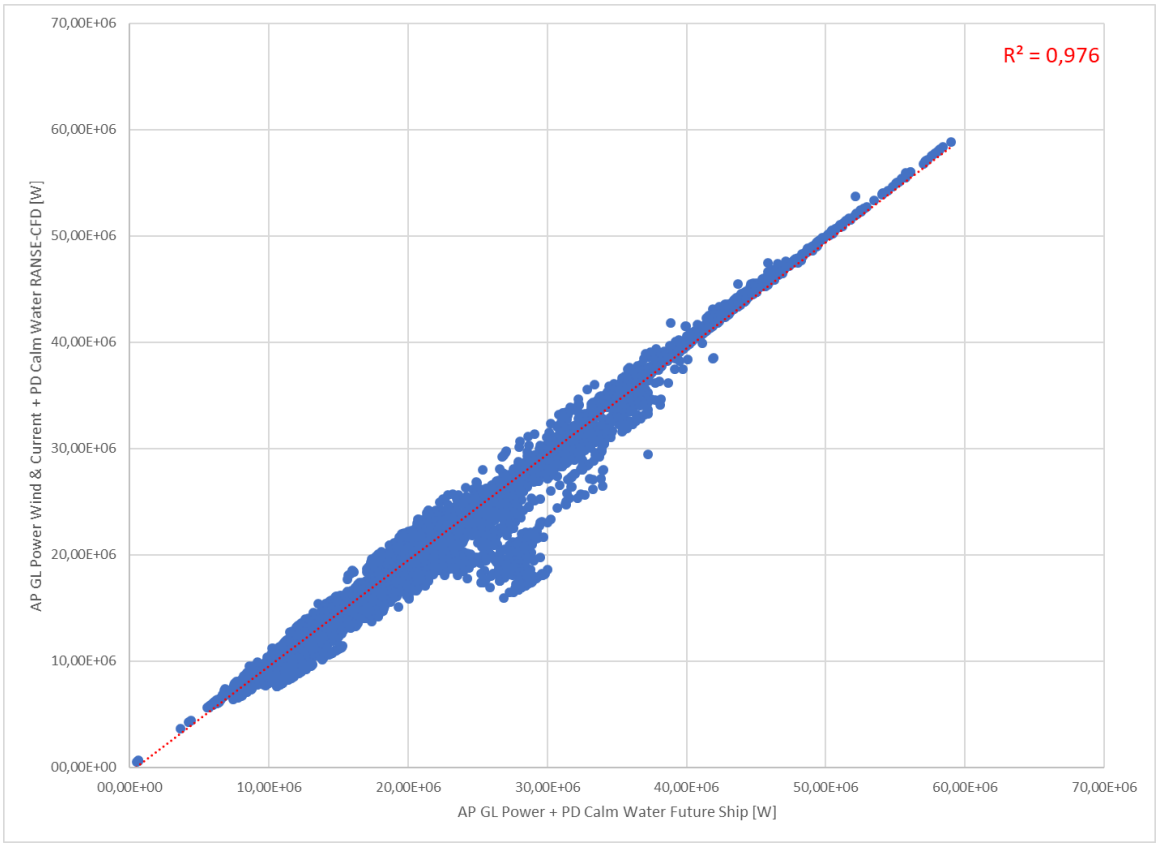


Figure 22 – Theoretical comparison of wind & current power (Case 6, y-axis) vs. total calculated power.

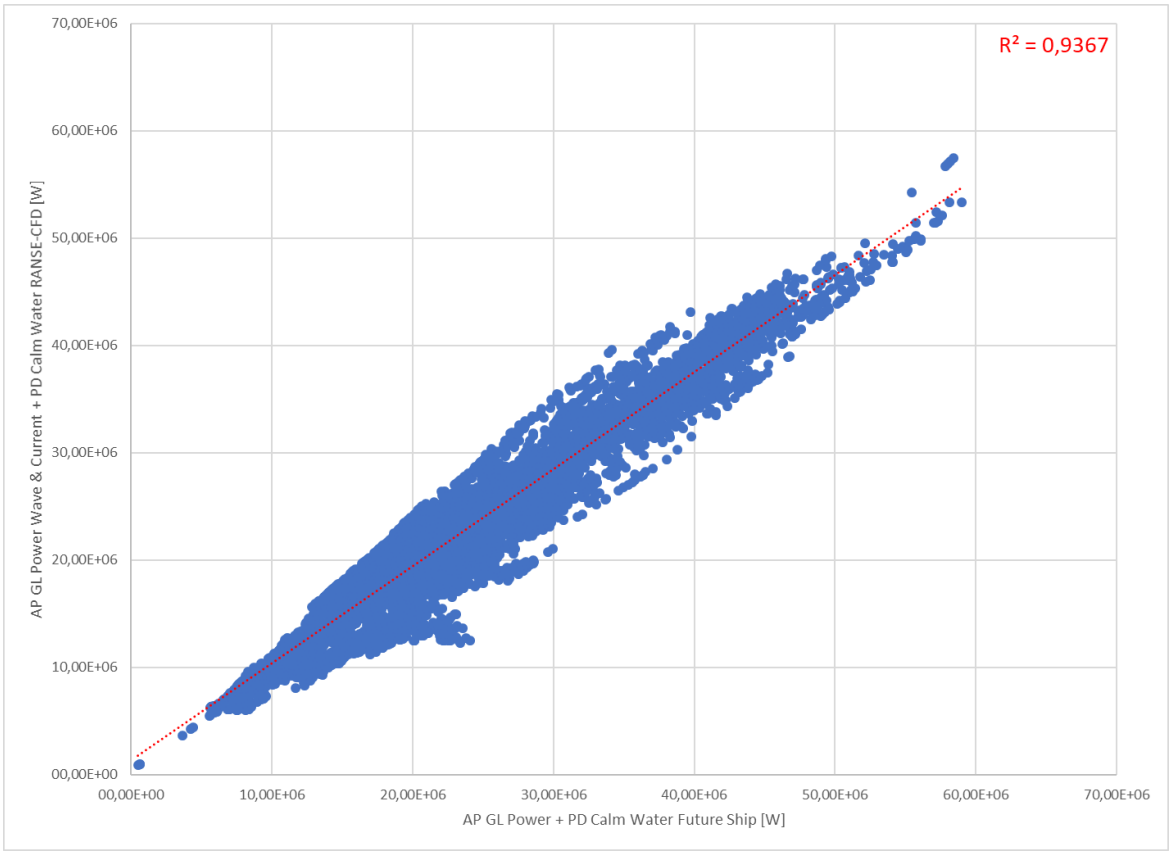


Figure 23 – Theoretical comparison of wave & current power (Case 7, y-axis) vs. total calculated power.

The table below summarizes the slope $\theta$ of the least square linear fit crossing origin.

Table 2 – Slope $\theta$ and $R^2$ of theoretical comparison.

| | Case 1 - Figure 17 | Case 2 - Figure 18 | Case 3 - Figure 19 | Case 4 - Figure 20 | Case 5 - Figure 21 | Case 6 - Figure 22 | Case 7 - Figure 23 |
|---|---|---|---|---|---|---|---|
| Slope $\theta$ | 0,945 | 0,980 | 0,956 | 0,944 | 1,001 | 0,979 | 0,956 |
| $R^2$ | 0,9179 | 0,9591 | 0,9152 | 0,9341 | 0,9771 | 0,976 | 0,9367 |

By analyzing the theoretical results in the light of slope shift, it is possible to conclude that wind (case 2) and wave (case 3) has a bigger influence on added power than current (case 4). However, those results should be further compared with real measurements to have a better understanding of the influencing parameters on added power.

## 5.3. Ratio of Computed to Measured Total Power

This attempt of analysis had as main goal to check the behaviour of the calculated and measured points on a ratio based graph. The ratio formula considered in this analysis is described in eq. (27).

$$\text{Ratio} = \frac{Power\ Calculated}{Power\ Measured} - 1{,}0 \tag{27}$$

This ratio would give us a sense of added power factors influence on total power by analysing how far the points are from axis 0. Moreover, from the ratios plots, it is possible to identify if there are any outliers that may distort the results.

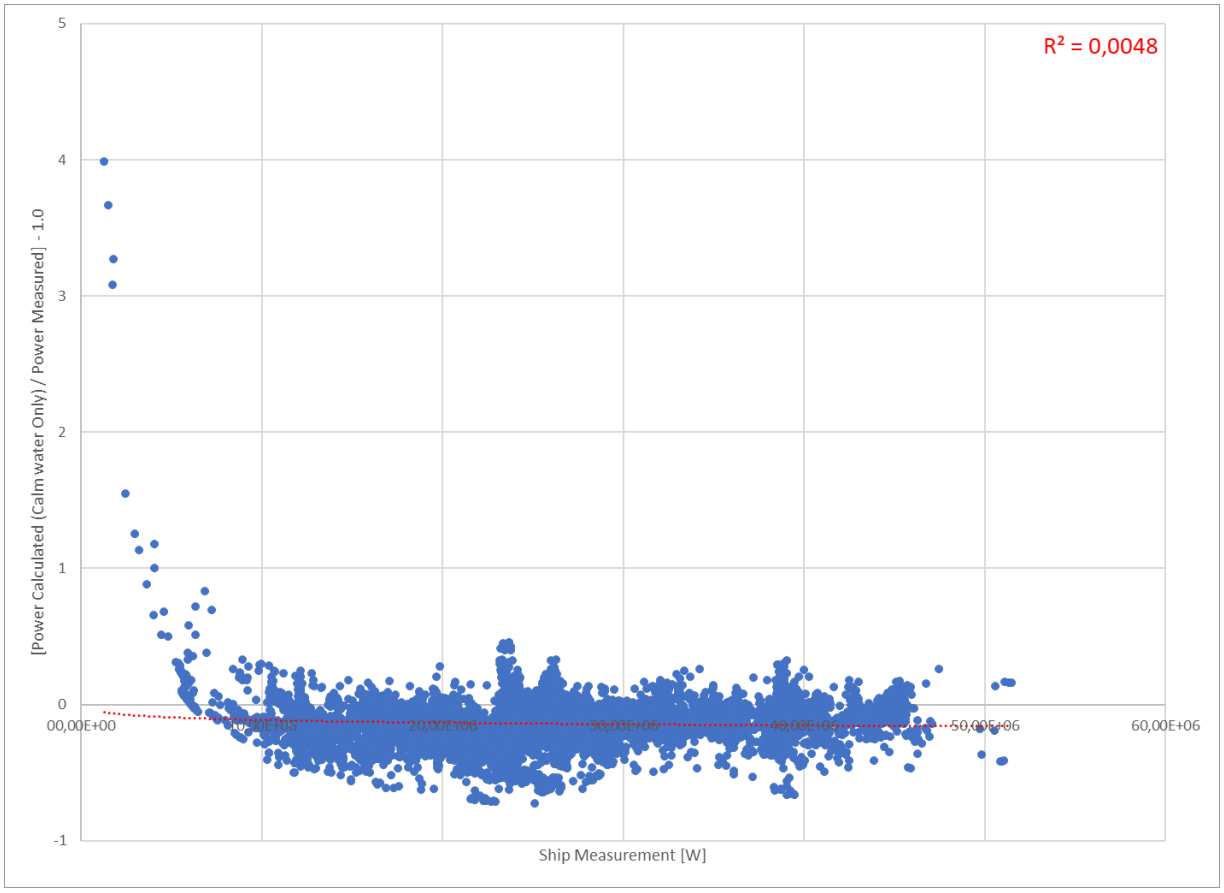


Figure 24 – Measured total power (x-axis) vs. calm-water power ratio (Case 1, y-axis).

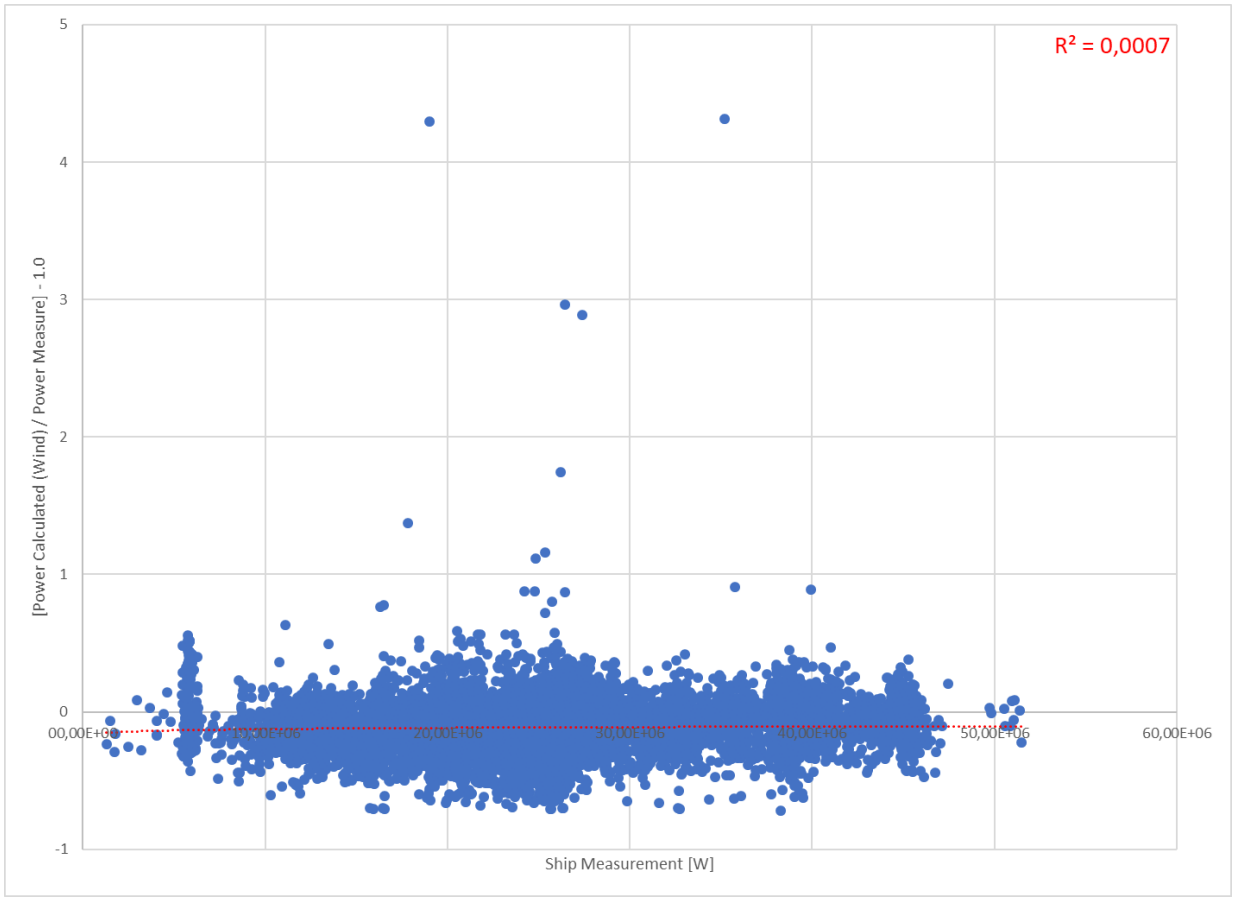


Figure 25 – Measured total power (x-axis) vs. wind power ratio (Case 2, y-axis).

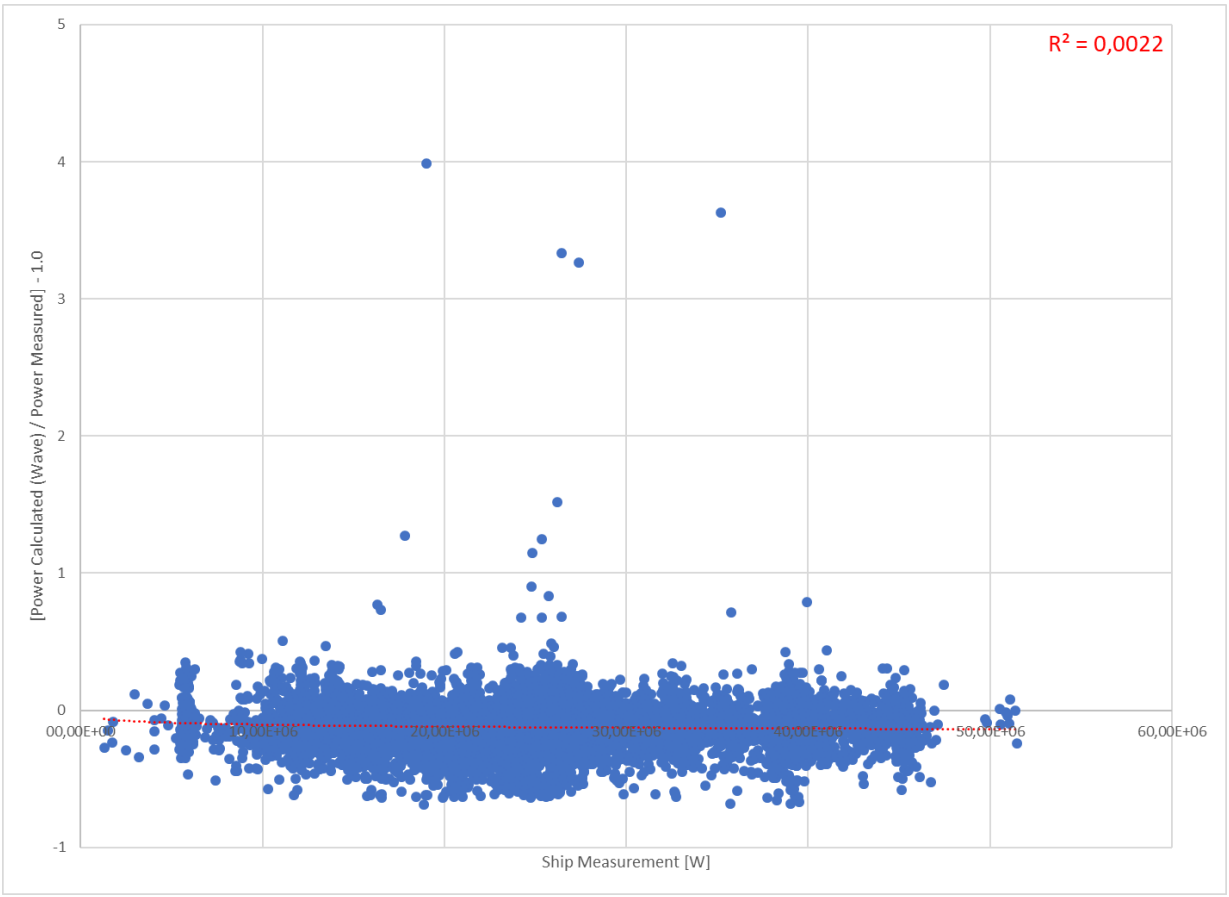


Figure 26 – Measured total power (x-axis) vs. wave power ratio (Case 3, y-axis).

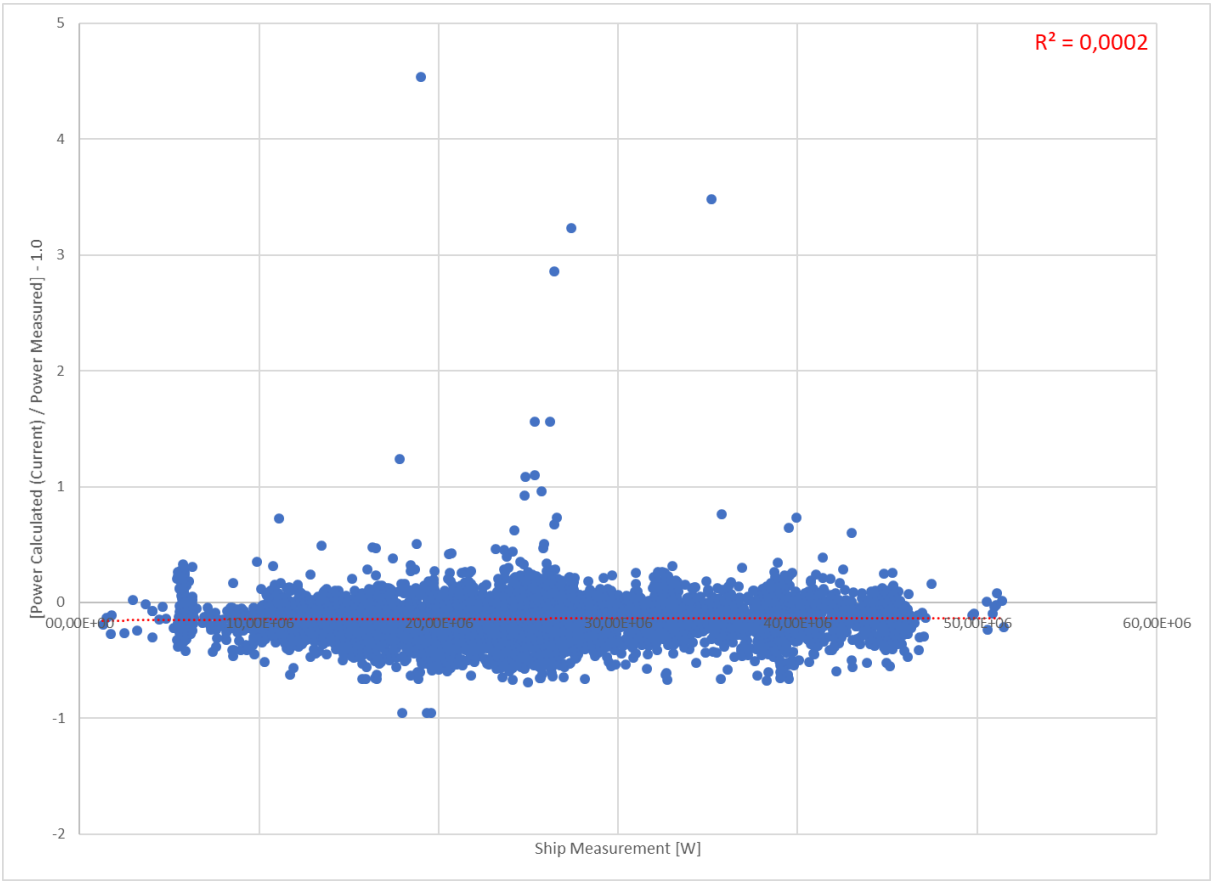


Figure 27 – Measured total power (x-axis) vs. current power ratio (Case 4, y-axis).

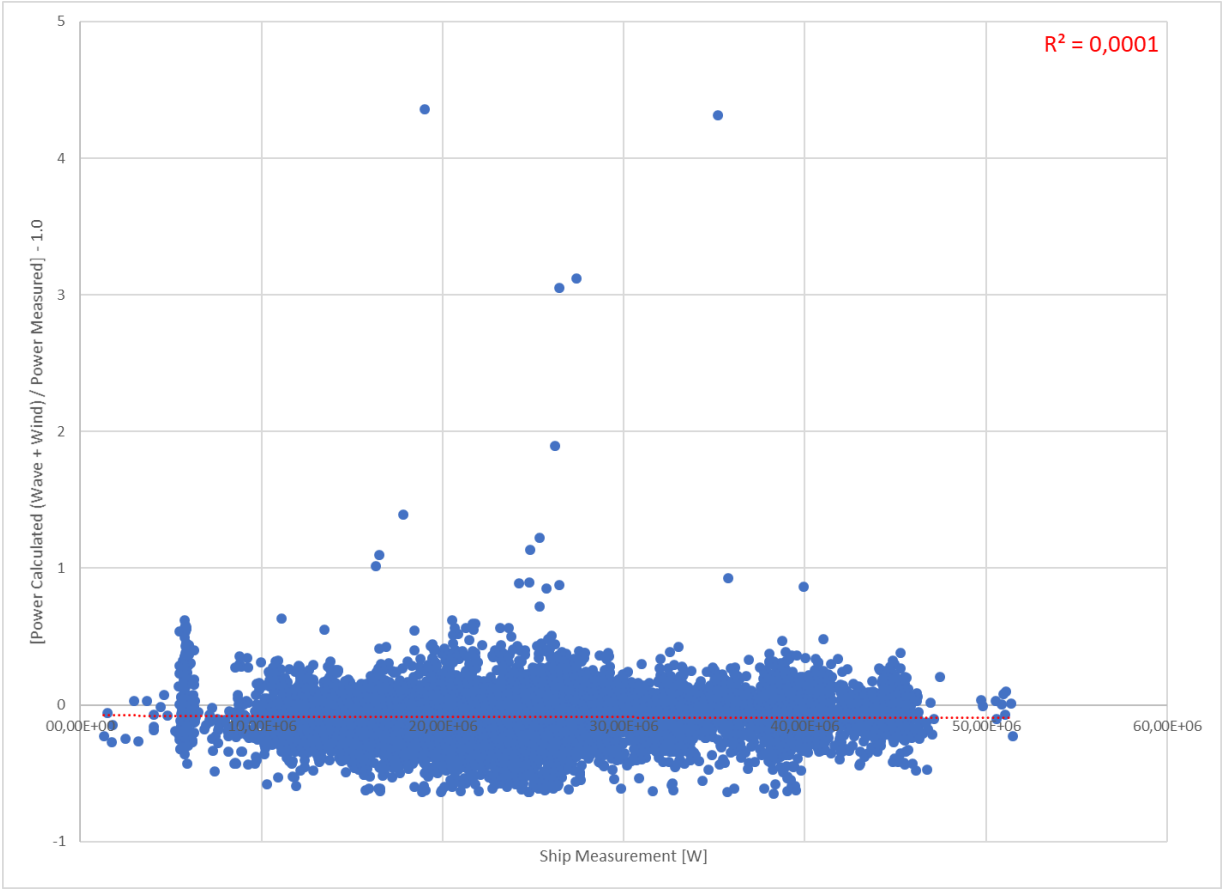


Figure 28 – Measured total power (x-axis) vs. wind & wave power ratio (Case 5, y-axis).

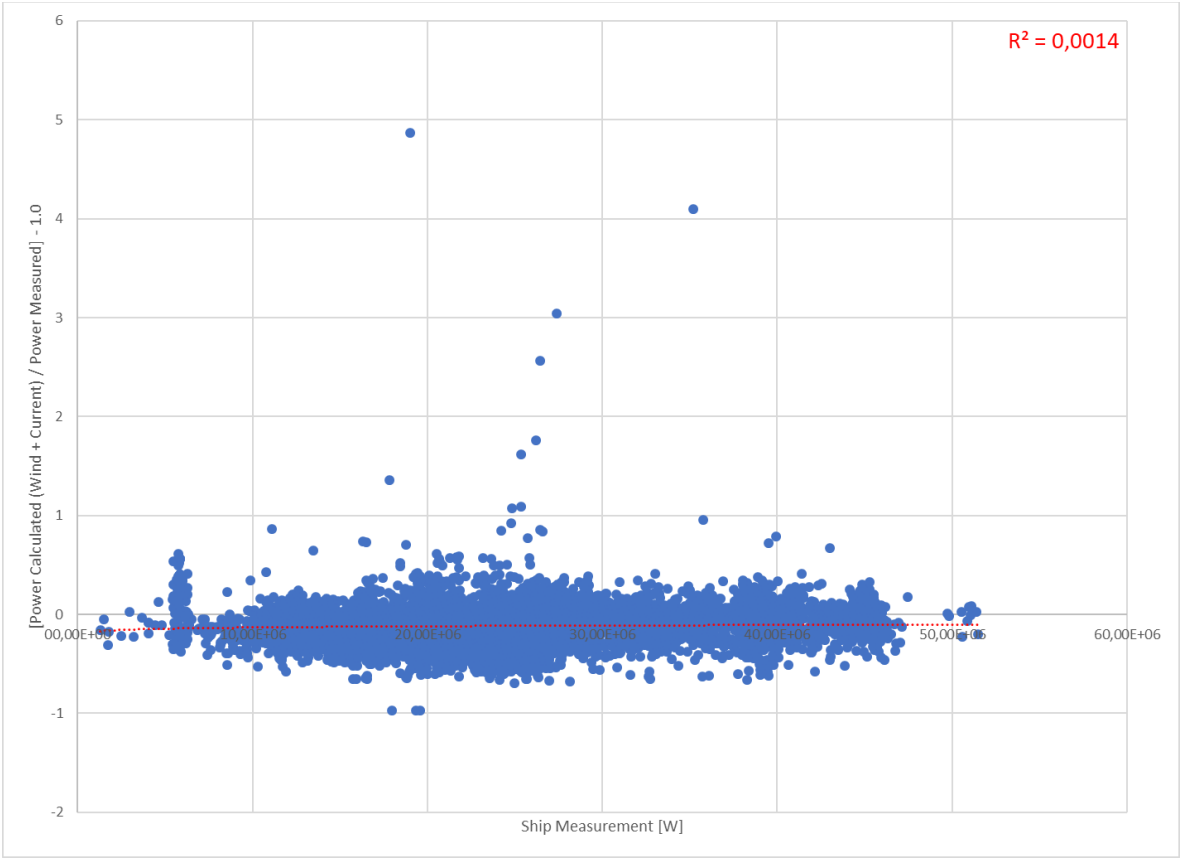


Figure 29 – Measured total power (x-axis) vs. wind & current power ratio (Case 6, y-axis).

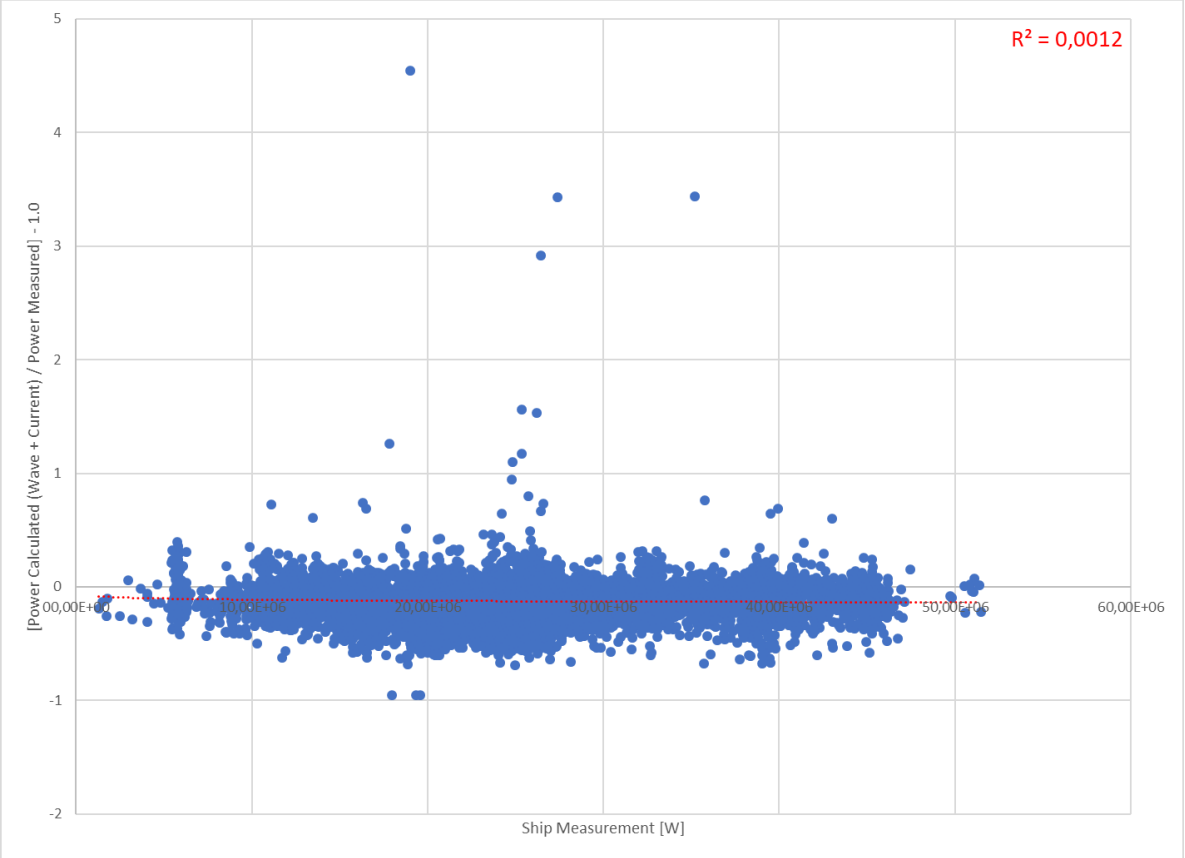


Figure 30 – Measured total power (x-axis) vs. wave & current power ratio (Case 7, y-axis).

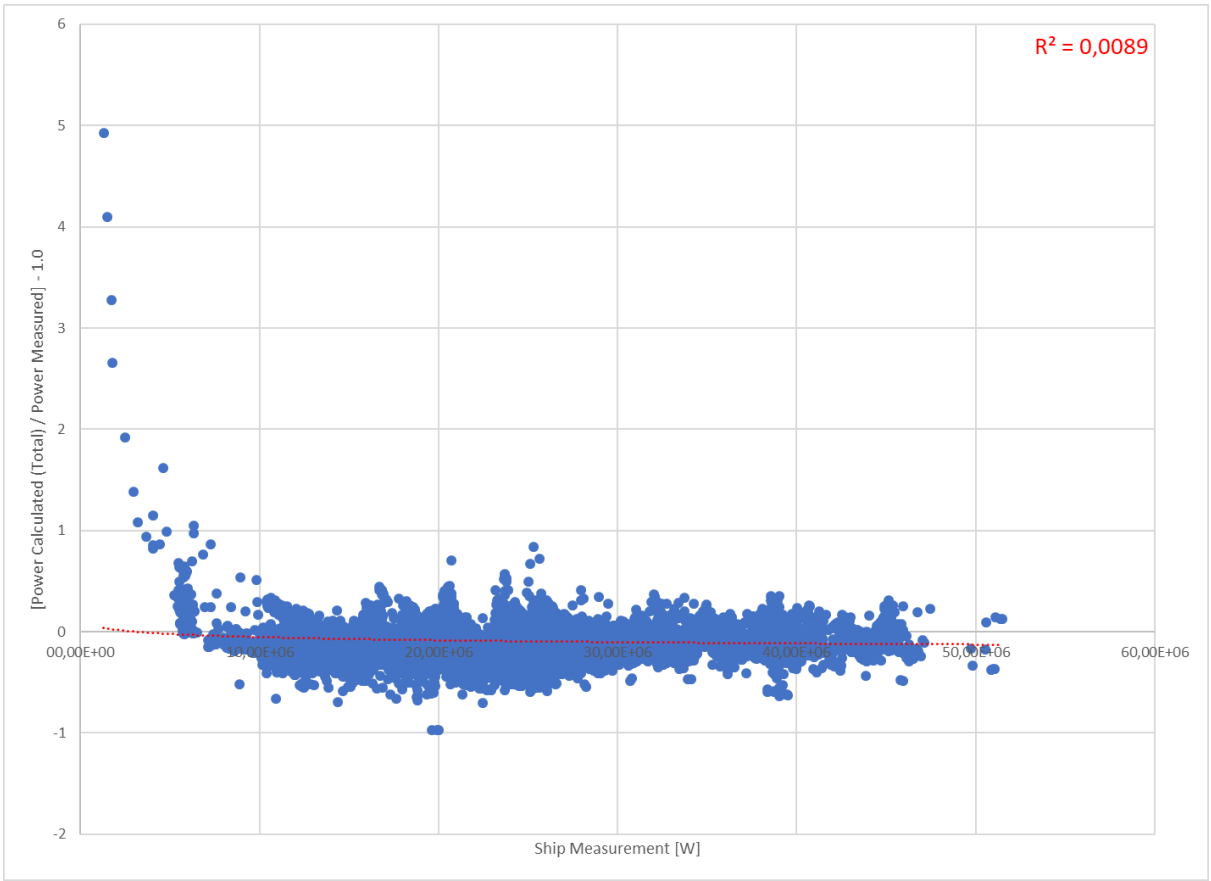


Figure 31 – Measured total power (x-axis) vs. total power computed ratio (Case 8, y-axis).

As expected it was possible to see that some points don't quite agree to the calculated power. However, the number of cases with a ratio bigger than 1,0 was about 9, which is less than 0,01% of the total cases studied, thus considered to have no influence on the final conclusions of this study.

## 5.4. Measured Total Power vs Calculated Added Power

In this approach it was observed the behaviour of the measurements against the calculated total power with the influence factors deducted. On those observations a linear regression was fit to get some sense of influence of the parameter by checking R-squared values. Figure 32 to Figure 38 illustrates the obtained results for such observations. Additionally, as proposed before, the slope shift $\theta$ from the ideal fit with slope 1,0 was calculated to support the sensitivity study.

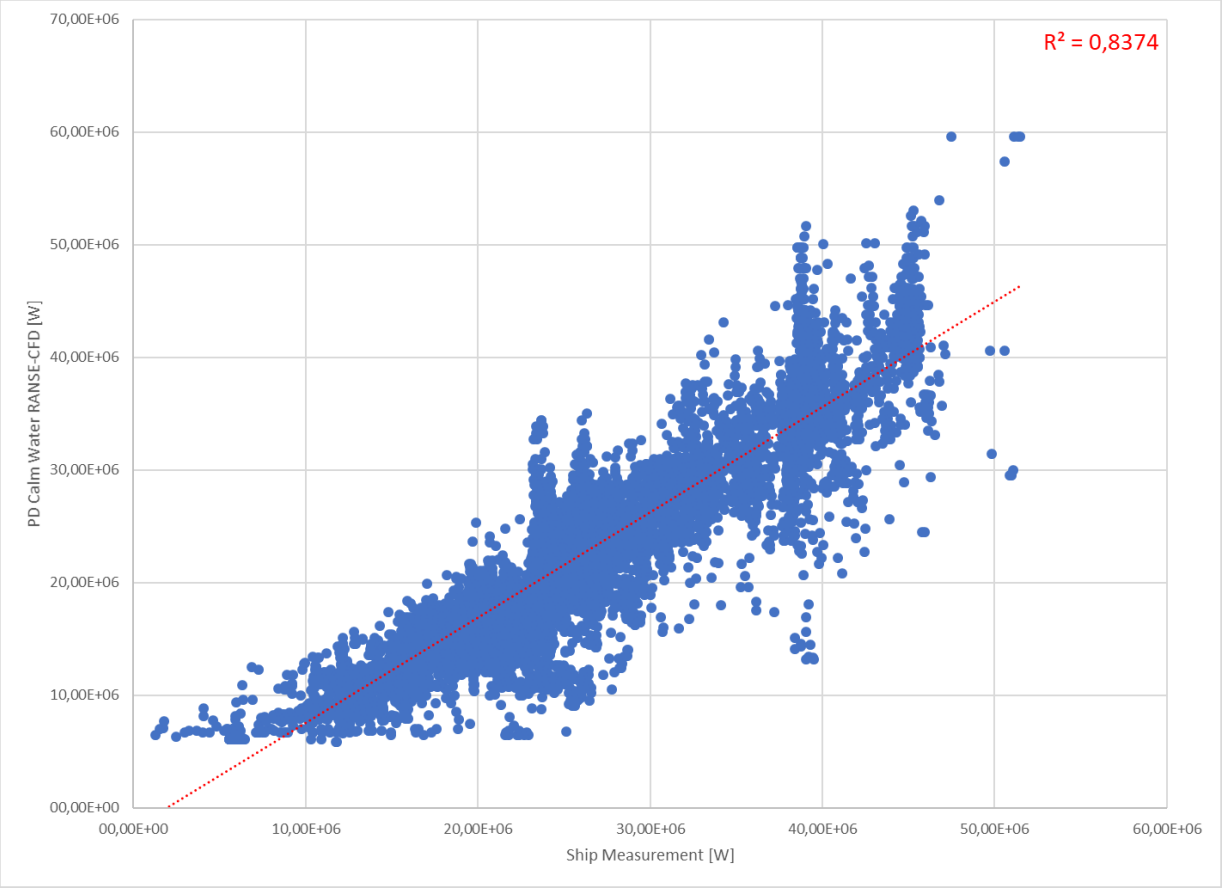


Figure 32 – Measured total power (x-axis) vs. computed calm-water power (Case 1, y-axis).

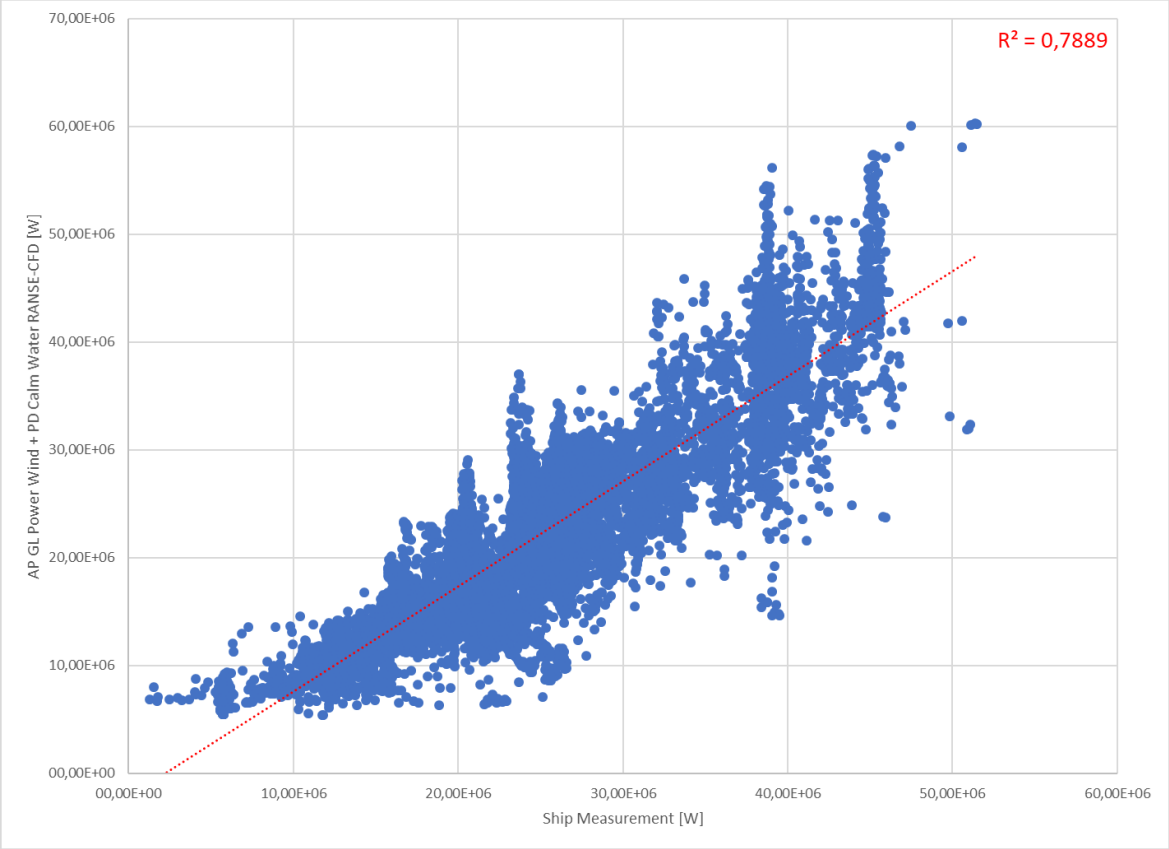


Figure 33 – Measured total power (x-axis) vs. computed wind power (Case 2, y-axis).

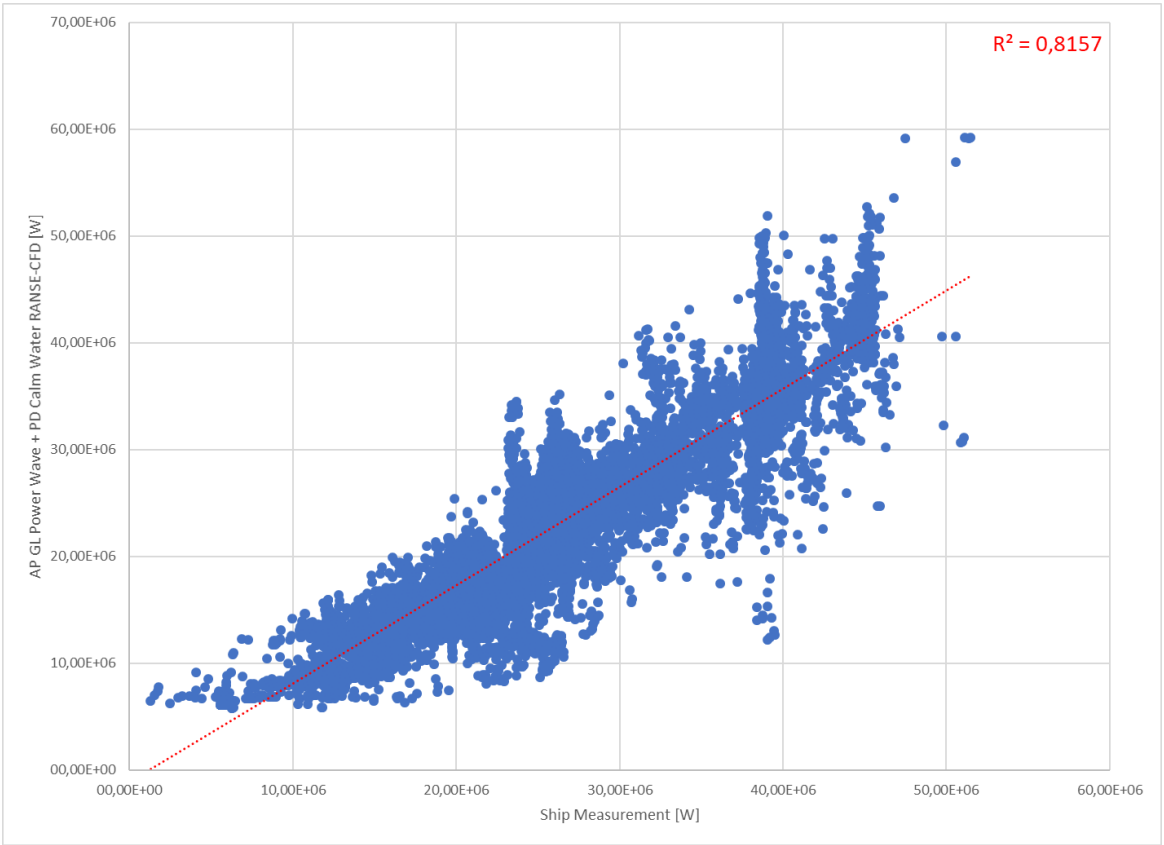


Figure 34 – Measured total power (x-axis) vs. computed wave power (Case 3, y-axis).

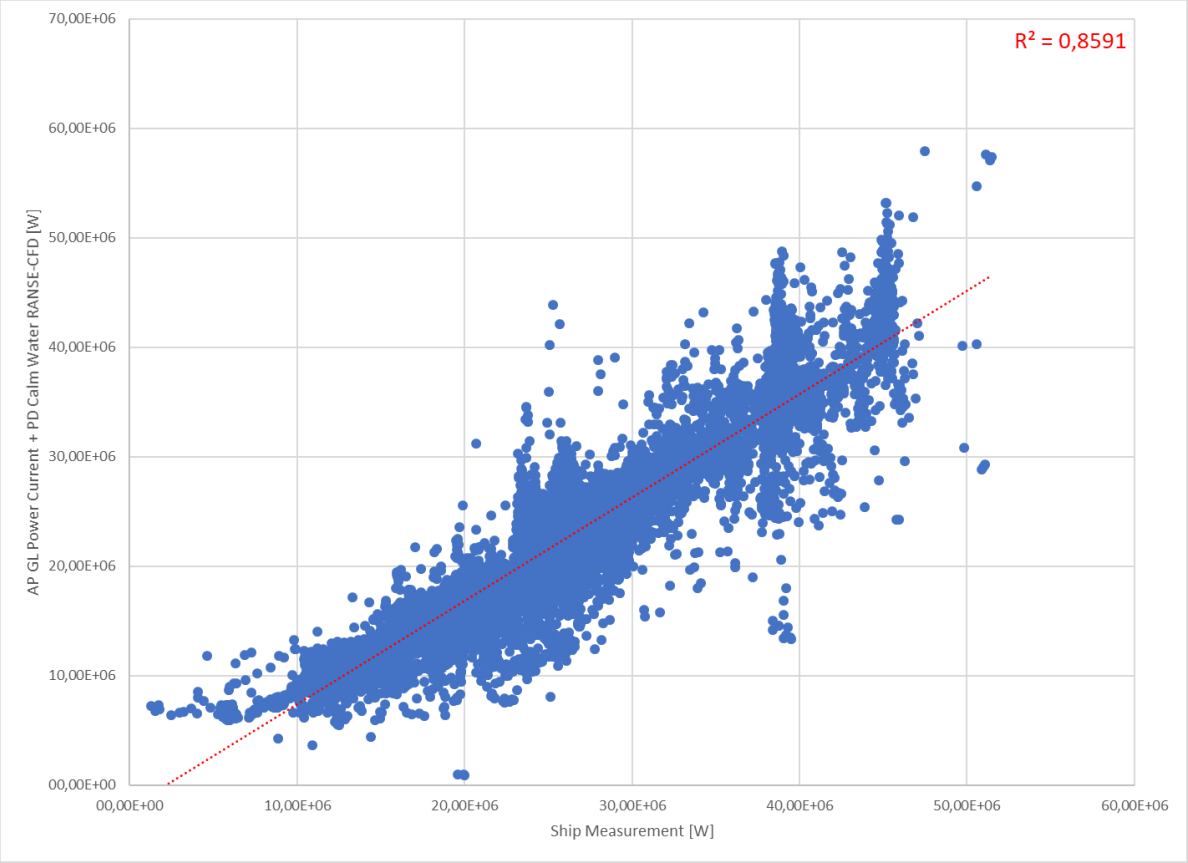


Figure 35 – Measured total power (x-axis) vs. computed current power (Case 4, y-axis).

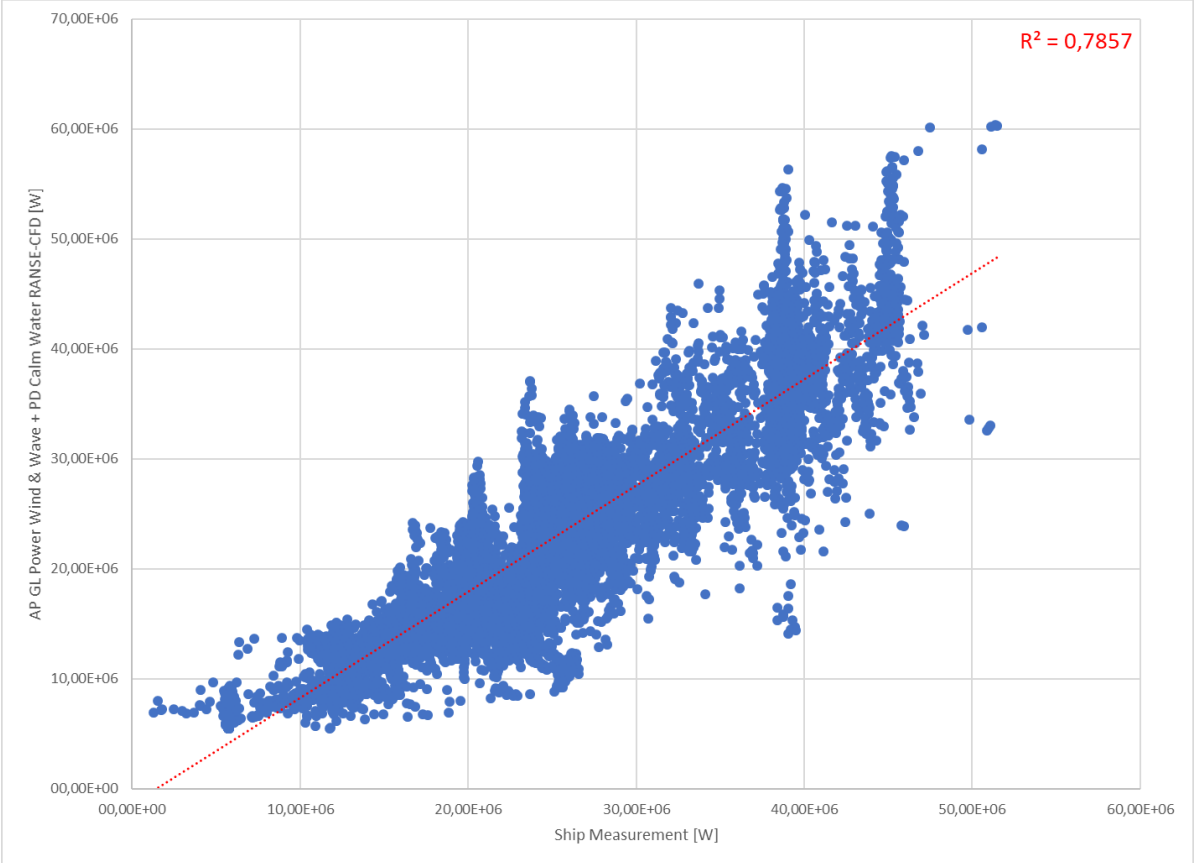


Figure 36 – Measured total power (x-axis) vs. computed wind & wave power (Case 5, y-axis).

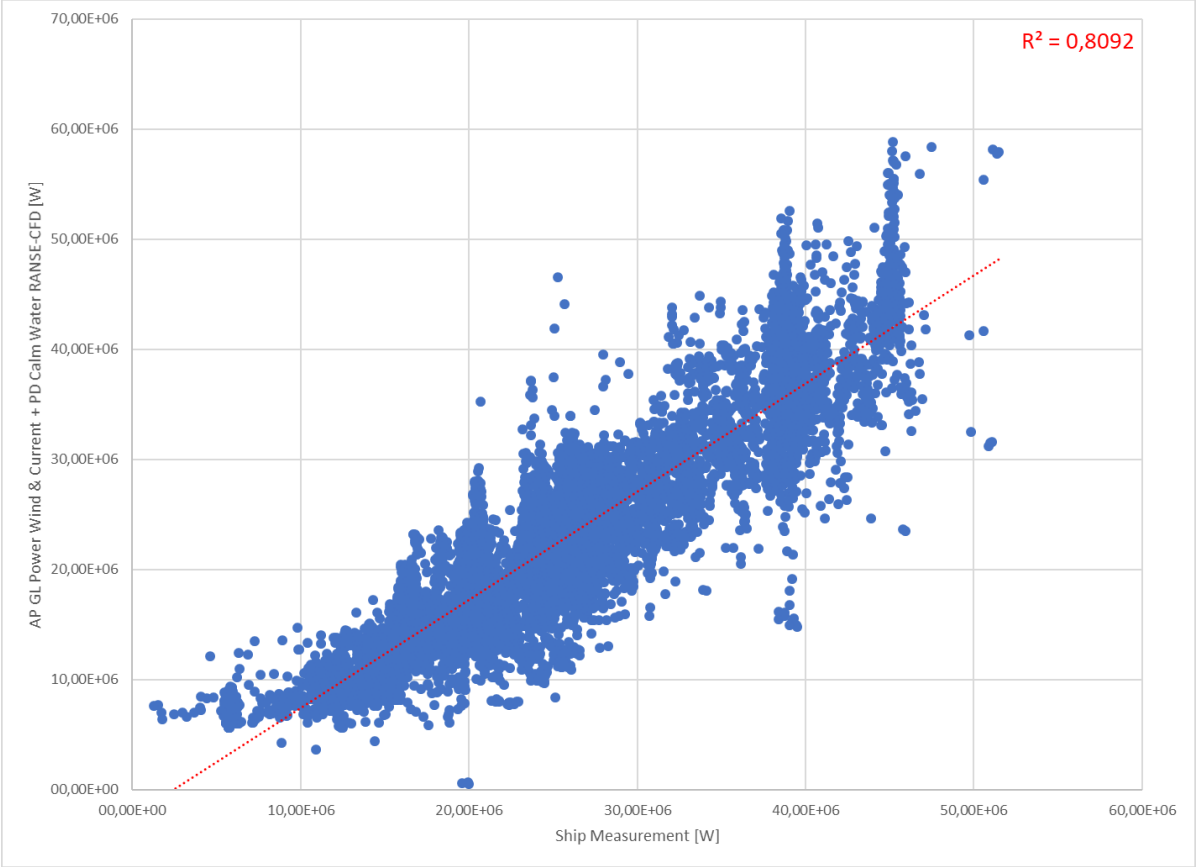


Figure 37 – Measured total power (x-axis) vs. computed wind & current power (Case 6, y-axis).

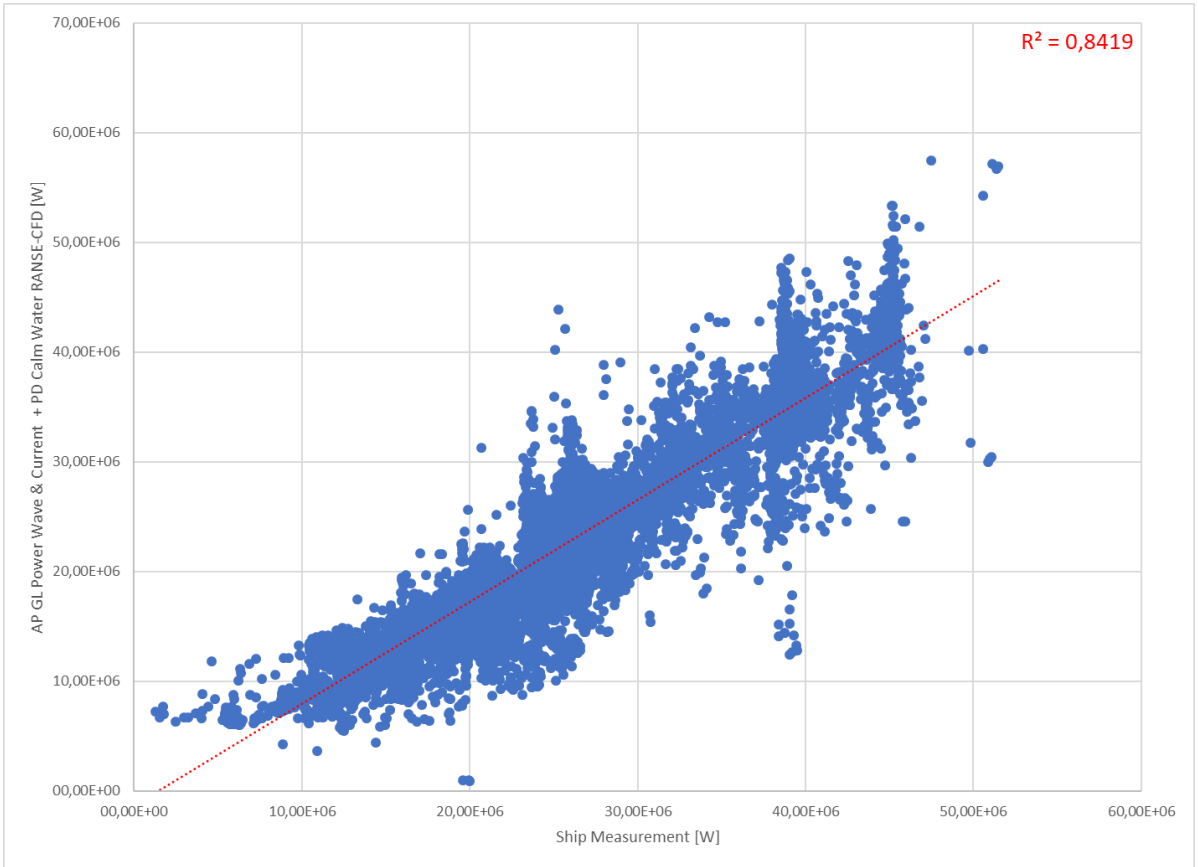


Figure 38 – Measured total power (x-axis) vs. computed wave & current power (Case 7, y-axis).

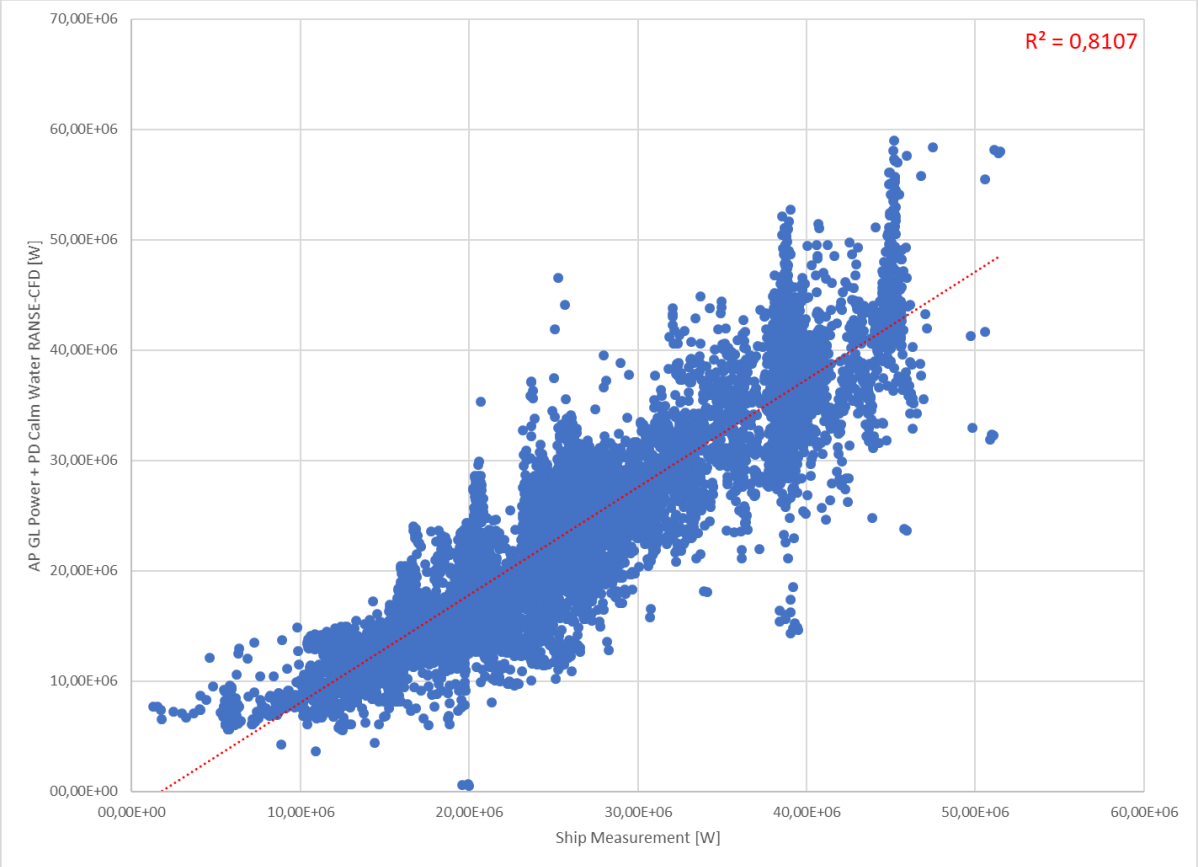


Figure 39 – Measured total power (x-axis) vs. computed total power (Case 8, y-axis).

Table 3 below, summarizes the shift in slope from the ideal fit as well as the $R^2$ from the best fit automatically generated by Microsoft Excel.

Table 3 – Slope $\theta$ and $R^2$ of measured vs. calculated total power.

| | Case 1 - Figure 32 | Case 2 - Figure 33 | Case 3 - Figure 34 | Case 4 - Figure 35 | Case 5 - Figure 36 | Case 6 - Figure 37 | Case 7 - Figure 38 | Case 8 - Figure 39 |
|---|---|---|---|---|---|---|---|---|
| Slope $\theta$ | 0,871 | 0,897 | 0,881 | 0,871 | 0,916 | 0,897 | 0,881 | 0,915 |
| $R^2$ | 0,8374 | 0,7889 | 0,8157 | 0,8591 | 0,7857 | 0,8092 | 0,8419 | 0,8107 |

It is possible to see from the table above that if we analyze the data from the shift of slope point of view, wind has a bigger contribution to added power (case 2), rather than wave (case 3) and current (case 4) respectively.

## 5.5. Measured Total Power X Calculated Added Power (By Classes)

From checking the graphs obtained above, one concern is that the linear regression might not be the best fit to analyse the influencing parameters on the total added power. Also, to have a clearer view of the results it would be nice to superimpose all plots. Unfortunately, with the amount of data available, superimposing the scatters is not practical.

It was decided to analyse the scatters by averaging the results by sectors. The graphs were averaged on five sectors based on ship speed and shaft power as shown in Table 4 and Table 5. Those ranges were equally divided based on the maximum and minimum values of the reported data in order to create five averaging sectors.

Table 4 – Speed ranges.

| Speed [knots] | |
|---|---|
| min | 13 |
| 13 | 16 |
| 16 | 19 |
| 19 | 22 |
| 22 | Max |

Table 5 – Shaft power ranges.

| Shaft Power [kW] | |
|---|---|
| min | 11.337 |
| 11.337 | 21.372 |
| 21.372 | 31.408 |
| 31.408 | 41.443 |
| 41.443 | Max |

Additionally, a histogram of the most common range of the analysed categories recorded in the ship report is shown in Figure 40 and Figure 41.

Those histograms aim to support the graphical analysis and make sure the study and conclusions take into considerations the relevance of the range verified. This means that the average values that fall in or nearby the most common operating ranges should have a bigger importance than the ones with lower number of occurrences.

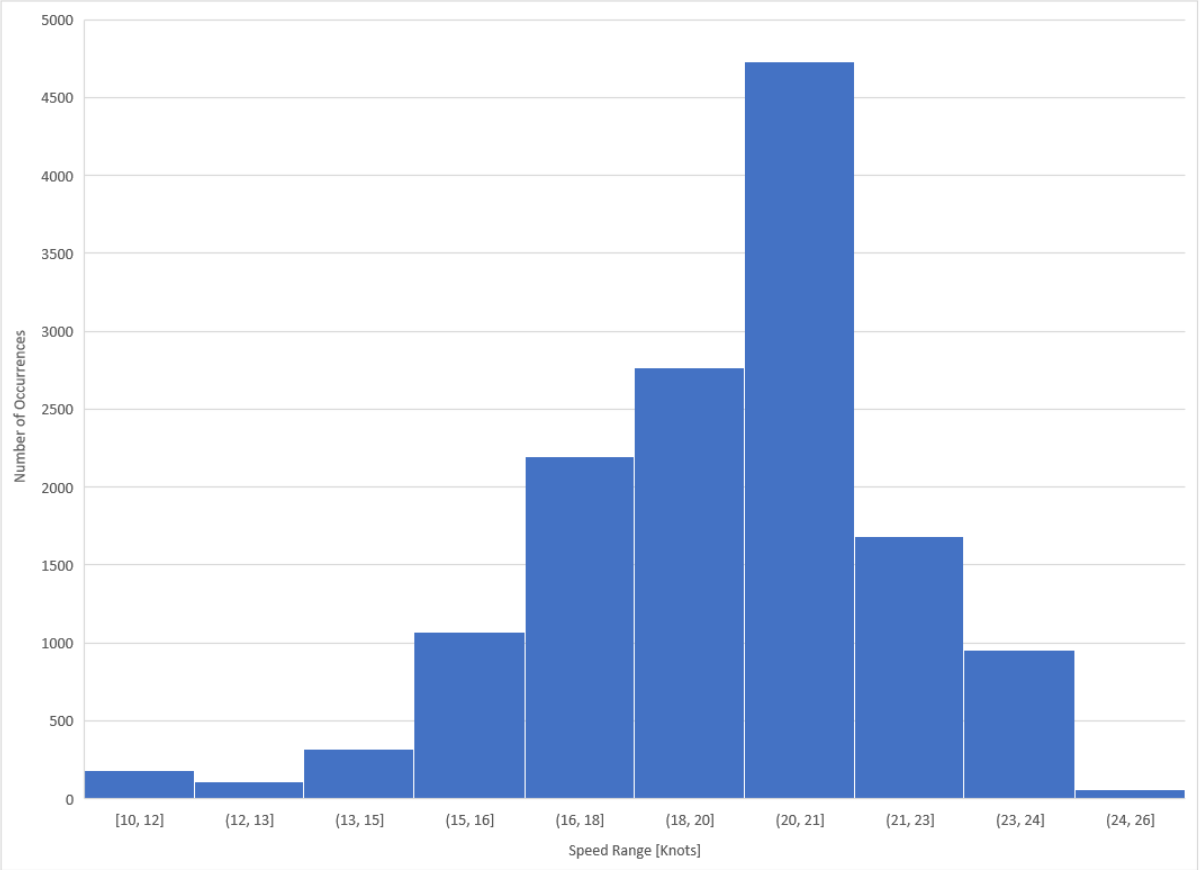


Figure 40 – Speed histogram.

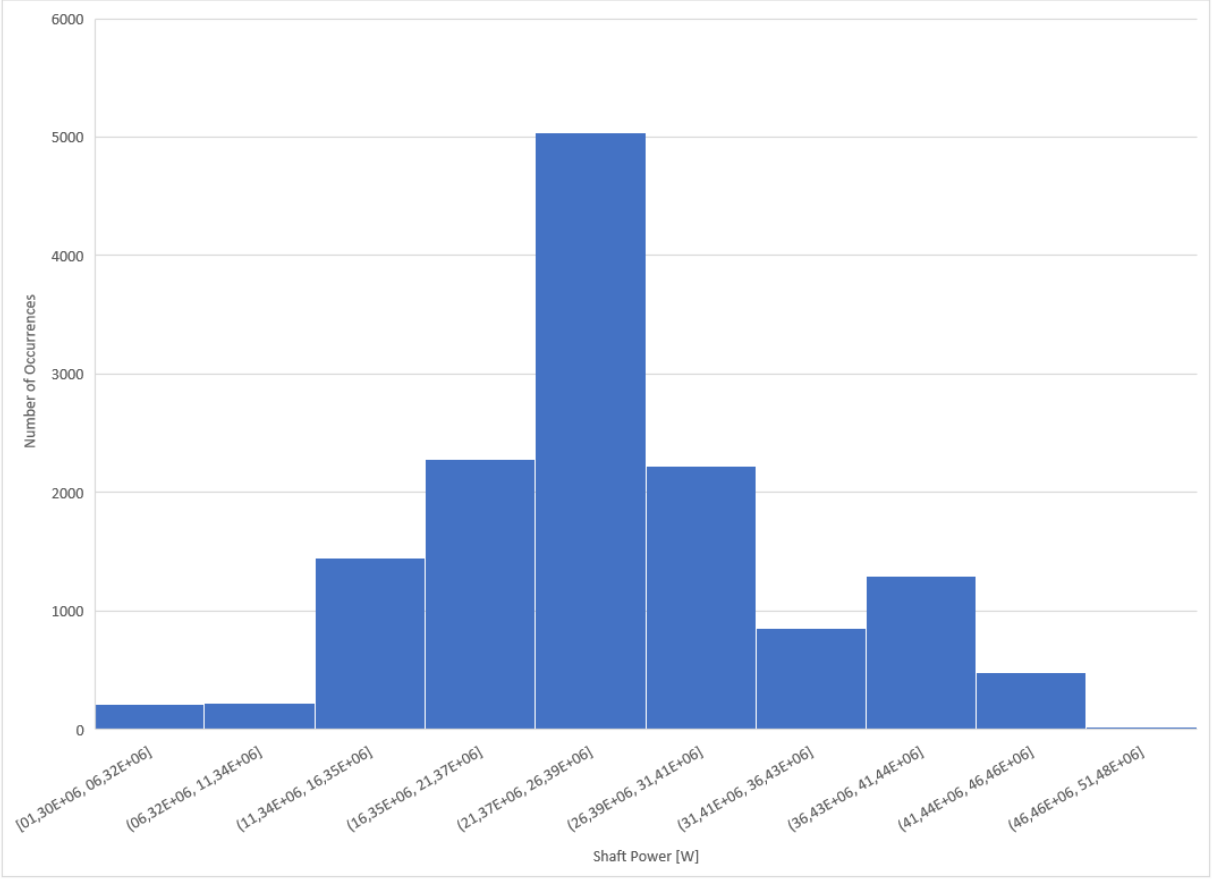


Figure 41 – Shaft power histogram.

### *5.5.1. Average Results Segregated by Speed*

The analysis below has considered an average of calculated power based on cases 1 to 8. Table 6 below, summarizes the average of the influencing factors (cases 1 to 4), whereas Figure 42, graphically illustrates those results.

Table 6 – Cases 1 to 4 average power by speed range.

| Range | | Average per range | | | | |
|---|---|---|---|---|---|---|
| Speed [Knots] | | PD Calm Water (Case 1) | PD Wind (Case 2) | PD Wave (Case 3) | PD Current (Case 4) | PD Total Measured |
| min | 13 | 06,50E+06 | 07,15E+06 | 06,66E+06 | 06,68E+06 | 07,62E+06 |
| 13 | 16 | 10,18E+06 | 10,34E+06 | 10,75E+06 | 10,28E+06 | 14,40E+06 |
| 16 | 19 | 15,21E+06 | 15,76E+06 | 15,48E+06 | 15,27E+06 | 19,54E+06 |
| 19 | 22 | 23,75E+06 | 24,17E+06 | 24,17E+06 | 23,71E+06 | 27,03E+06 |
| 22 | max | 37,80E+06 | 39,60E+06 | 37,71E+06 | 37,52E+06 | 39,64E+06 |

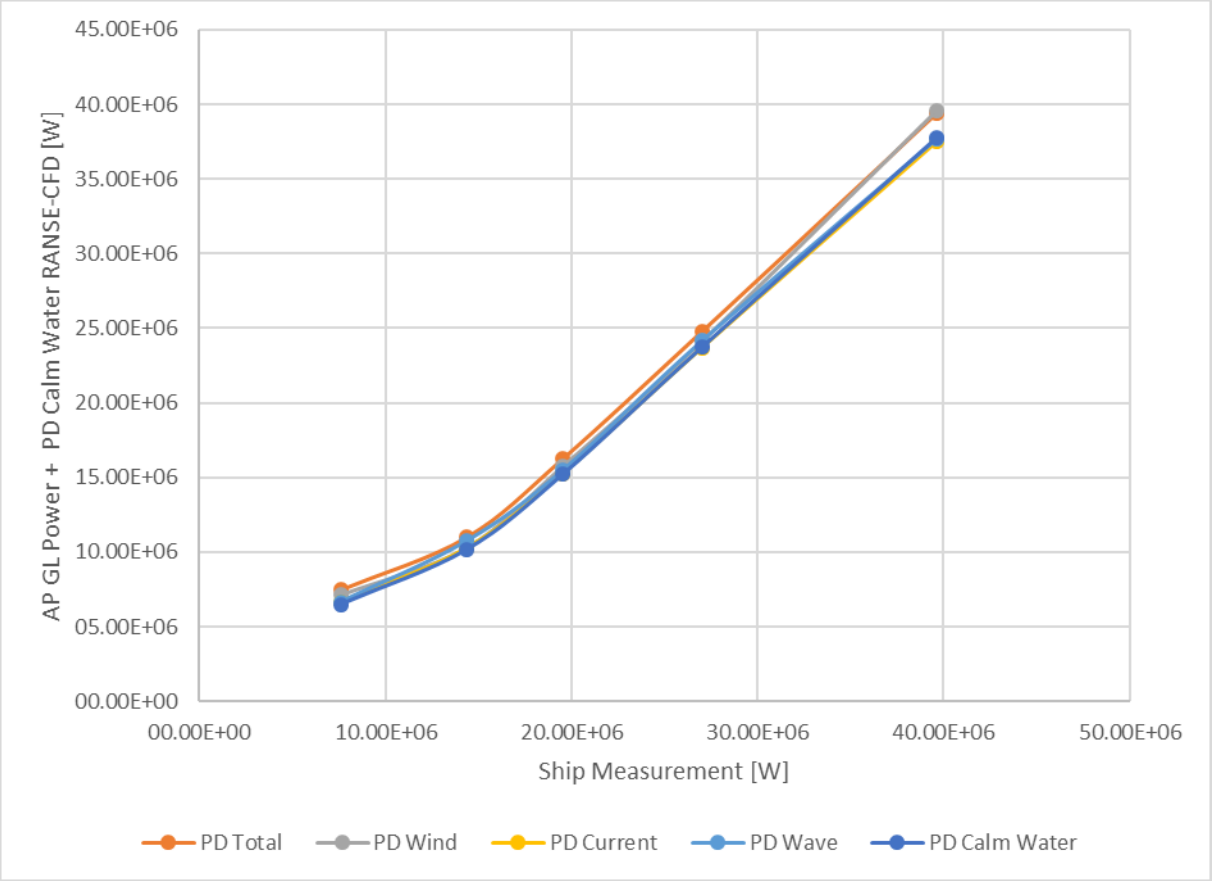


Figure 42 – Cases 1 to 4 - distributed over ship speed.

Table 7 – Cases 5 to 8 average power by speed range.

| Range | | Average per range | | | | |
|---|---|---|---|---|---|---|
| Speed [Knots] | | PD Wind & Wave (Case 5) | PD Wind & Current (Case 6) | PD Wave & Current (Case 7) | PD Total Calculated (Case 8) | PD Total Measured |
| min | 13 | 07,31E+06 | 07,33E+06 | 06,84E+06 | 07,49E+06 | 07,62E+06 |
| 13 | 16 | 10,94E+06 | 10,44E+06 | 10,84E+06 | 11,02E+06 | 14,40E+06 |
| 16 | 19 | 16,21E+06 | 15,83E+06 | 15,53E+06 | 16,27E+06 | 19,54E+06 |
| 19 | 22 | 24,88E+06 | 24,12E+06 | 24,12E+06 | 24,83E+06 | 27,03E+06 |
| 22 | max | 39,73E+06 | 39,31E+06 | 37,43E+06 | 39,44E+06 | 39,64E+06 |

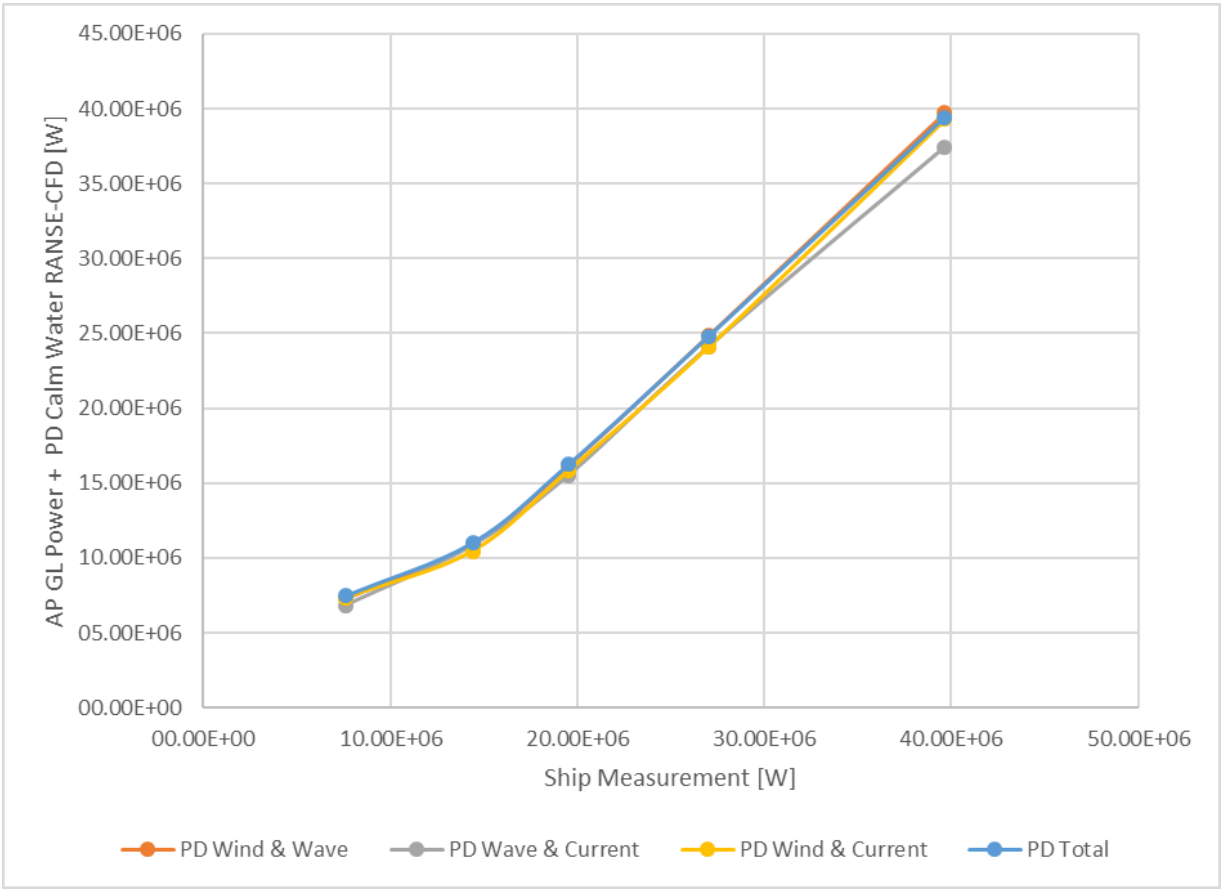


Figure 43 – Cases 5 to 8 – distributed over speed.

Table 8 – Cases 1 to 4 average ratio by speed range.

| Range | | Average Ratio per Range | | | | |
|---|---|---|---|---|---|---|
| Speed [Knots] | | PD Calm Water (Case 1) | PD Wind (Case 2) | PD Wave (Case 3) | PD Current (Case 4) | PD Total Measured |
| min | 13 | 0,85 | 0,94 | 0,87 | 0,88 | 03,40E+06 |
| 13 | 16 | 0,71 | 0,72 | 0,75 | 0,71 | 07,26E+06 |
| 16 | 19 | 0,78 | 0,81 | 0,79 | 0,78 | 15,71E+06 |
| 19 | 22 | 0,88 | 0,89 | 0,89 | 0,88 | 25,10E+06 |
| 22 | max | 0,95 | 1,00 | 0,95 | 0,95 | 38,85E+06 |

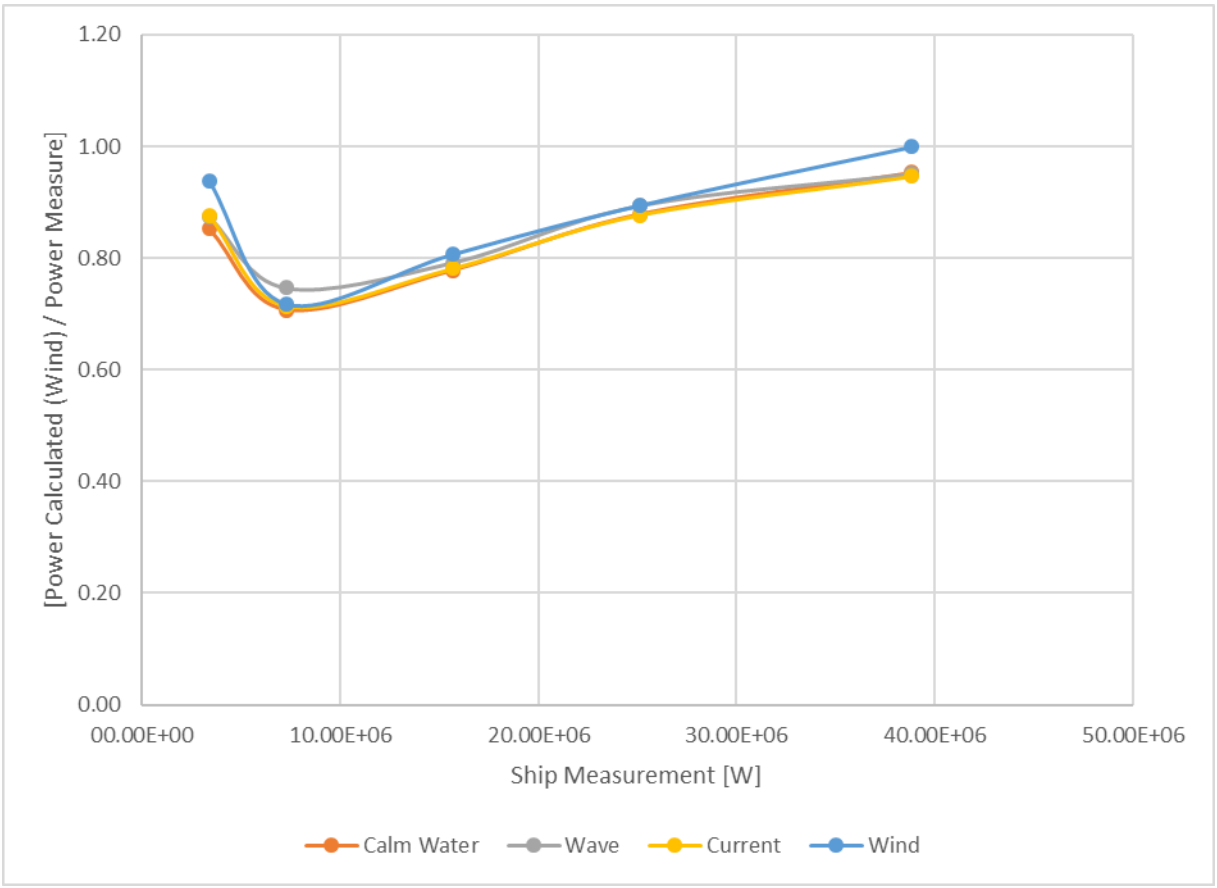


Figure 44 – Cases 1 to 4 ratio - distributed over speed.

Table 9 – Cases 5 to 8 average ratio by speed range.

| Range | | Average Ratio per Range | | | | |
|---|---|---|---|---|---|---|
| Speed [Knots] | | PD Wind & Wave (Case 5) | PD Wind & Current (Case 6) | PD Wave & Current (Case 7) | PD Total Calculated (Case 8) | PD Total Measured |
| min | 13 | 0,96 | 0,96 | 0,90 | 0,98 | 03,40E+06 |
| 13 | 16 | 0,76 | 0,72 | 0,75 | 0,77 | 07,26E+06 |
| 16 | 19 | 0,83 | 0,81 | 0,80 | 0,83 | 15,71E+06 |
| 19 | 22 | 0,92 | 0,89 | 0,89 | 0,92 | 25,10E+06 |
| 22 | max | 1,00 | 0,99 | 0,94 | 0,99 | 38,85E+06 |

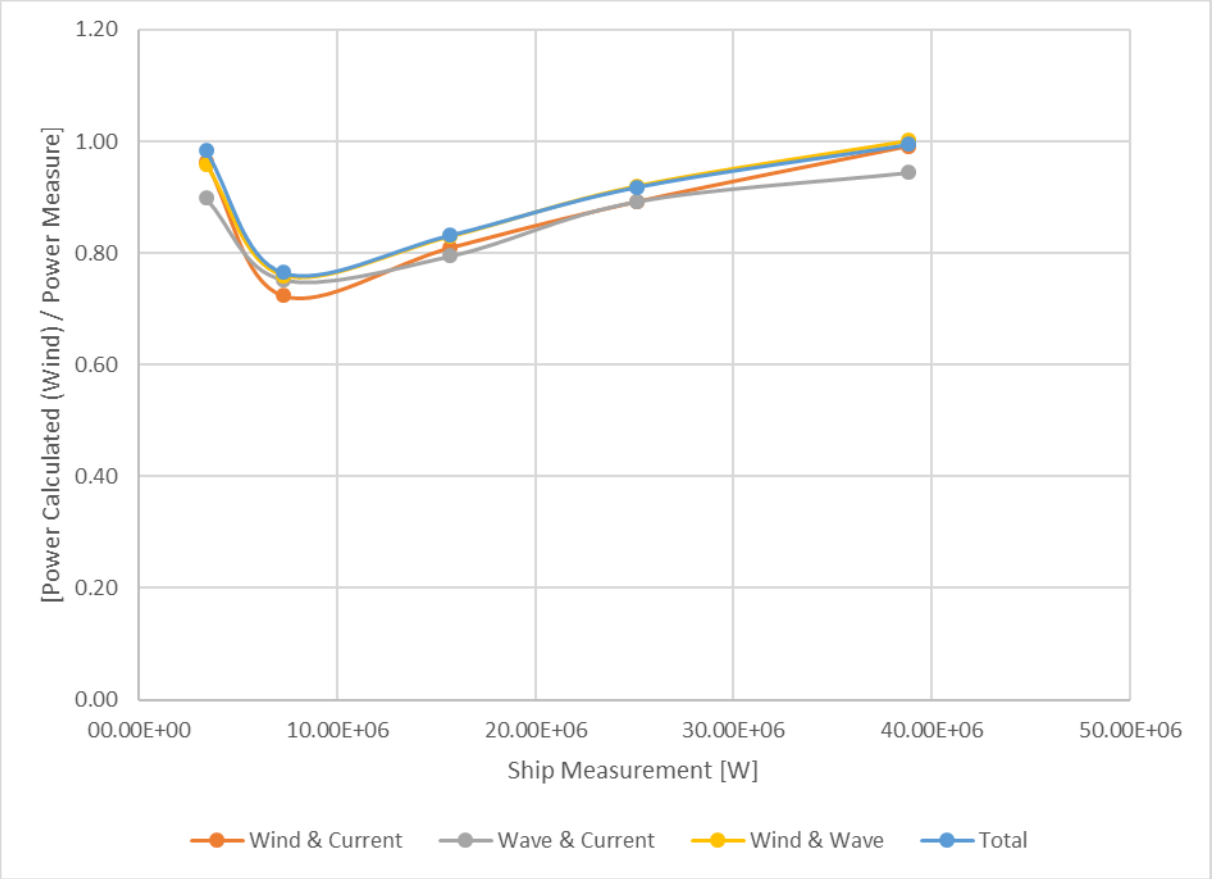


Figure 45 – Cases 5 to 8 ratio - distributed over speed.

From the graphs and tables shown on this sub-chapter, it is possible to see that depending on the range analyzed, the averaging value varies. In this sense it would be confusing to say what parameter has the most influence on the total power. However, if we have a closer look on the most common range of speed [19 knots ~ 22 knots], it is possible to conclude that the bigger influencing parameter are wind, wave and current respectively.

### *5.5.2. Average Results Segregated by Shaft Power*

In this sub-item, the analyses were performed by segregating the results based on the shaft Power. The most common range of operating power reported by the ship owner and shown by the histogram on Figure 41 was [21,37 MW ~ 26,39 MW]. Thus, the enveloping range of [21.372 kW ~ 31.408 kW] were highlighted on the further tables.

Table 10 – Cases 1 to 4 average power by shaft power range.

| Range | | Average per range | | | | |
|---|---|---|---|---|---|---|
| Shaft Power [kW] | | PD Calm Water (Case 1) | PD Wind (Case 2) | PD Wave (Case 3) | PD Current (Case 4) | PD Total Measured |
| min | 11.337 | 07,82E+06 | 08,14E+06 | 08,02E+06 | 07,69E+06 | 07,75E+06 |
| 11.337 | 21.372 | 14,03E+06 | 14,71E+06 | 14,41E+06 | 13,89E+06 | 17,10E+06 |
| 21.372 | 31.408 | 21,98E+06 | 22,29E+06 | 22,40E+06 | 21,95E+06 | 25,63E+06 |
| 31.408 | 41.443 | 33,02E+06 | 34,37E+06 | 33,06E+06 | 33,26E+06 | 36,93E+06 |
| 41.443 | max | 40,79E+06 | 42,38E+06 | 40,45E+06 | 40,48E+06 | 44,39E+06 |

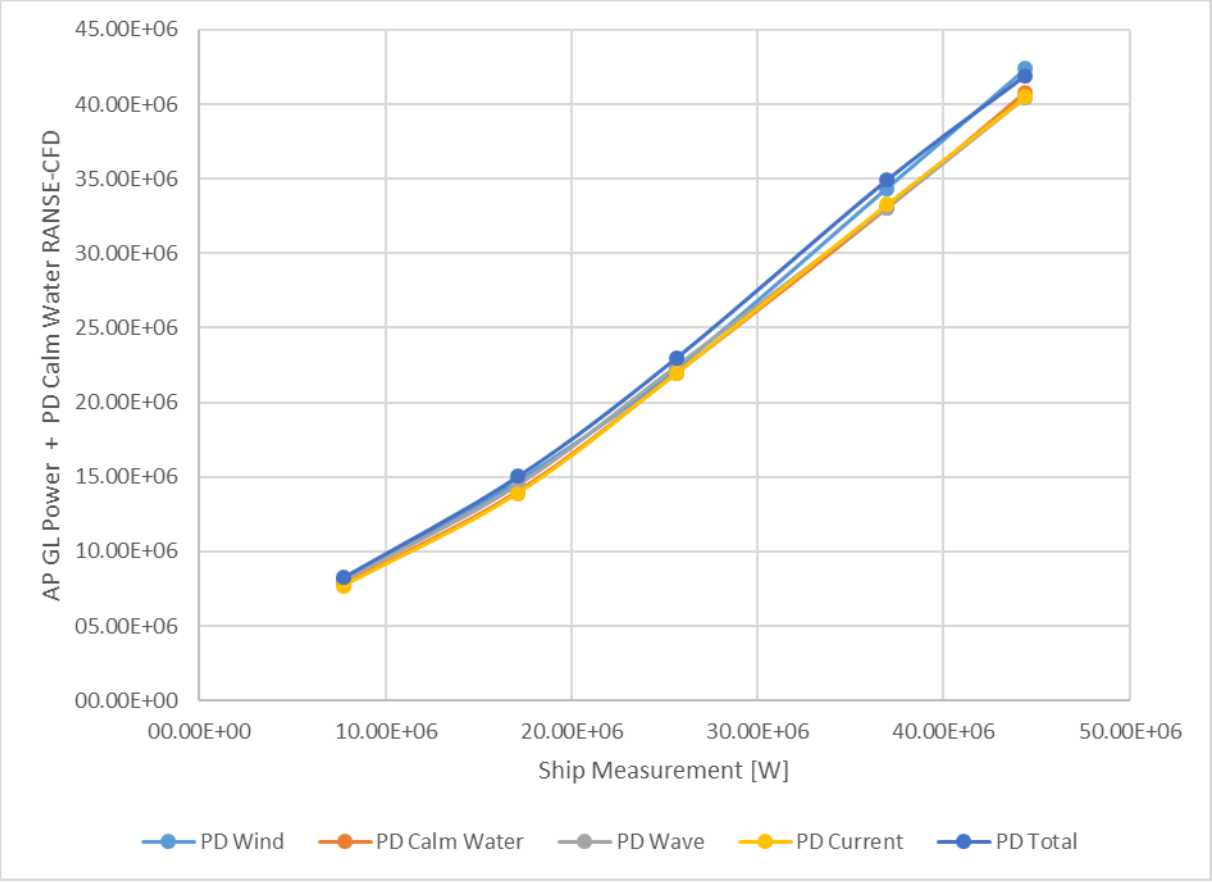


Figure 46 – Cases 1 to 4 - distributed over shaft power.

Table 11 – Cases 5 to 8 average power by shaft power range.

| Range | | Average per range | | | | |
|---|---|---|---|---|---|---|
| Shaft Power [kW] | | PD Wind & Wave (Case 5) | PD Wind & Current (Case 6) | PD Wave & Current (Case 7) | PD Total Calculated (Case 8) | PD Total Measured |
| min | 11.337 | 08,40E+06 | 08,02E+06 | 07,88E+06 | 08,27E+06 | 07,75E+06 |
| 11.337 | 21.372 | 15,18E+06 | 14,57E+06 | 14,26E+06 | 15,03E+06 | 17,10E+06 |
| 21.372 | 31.408 | 23,01E+06 | 22,27E+06 | 22,37E+06 | 22,98E+06 | 25,63E+06 |
| 31.408 | 41.443 | 34,67E+06 | 34,60E+06 | 33,30E+06 | 34,90E+06 | 36,93E+06 |
| 41.443 | max | 42,24E+06 | 42,05E+06 | 40,13E+06 | 41,92E+06 | 44,39E+06 |

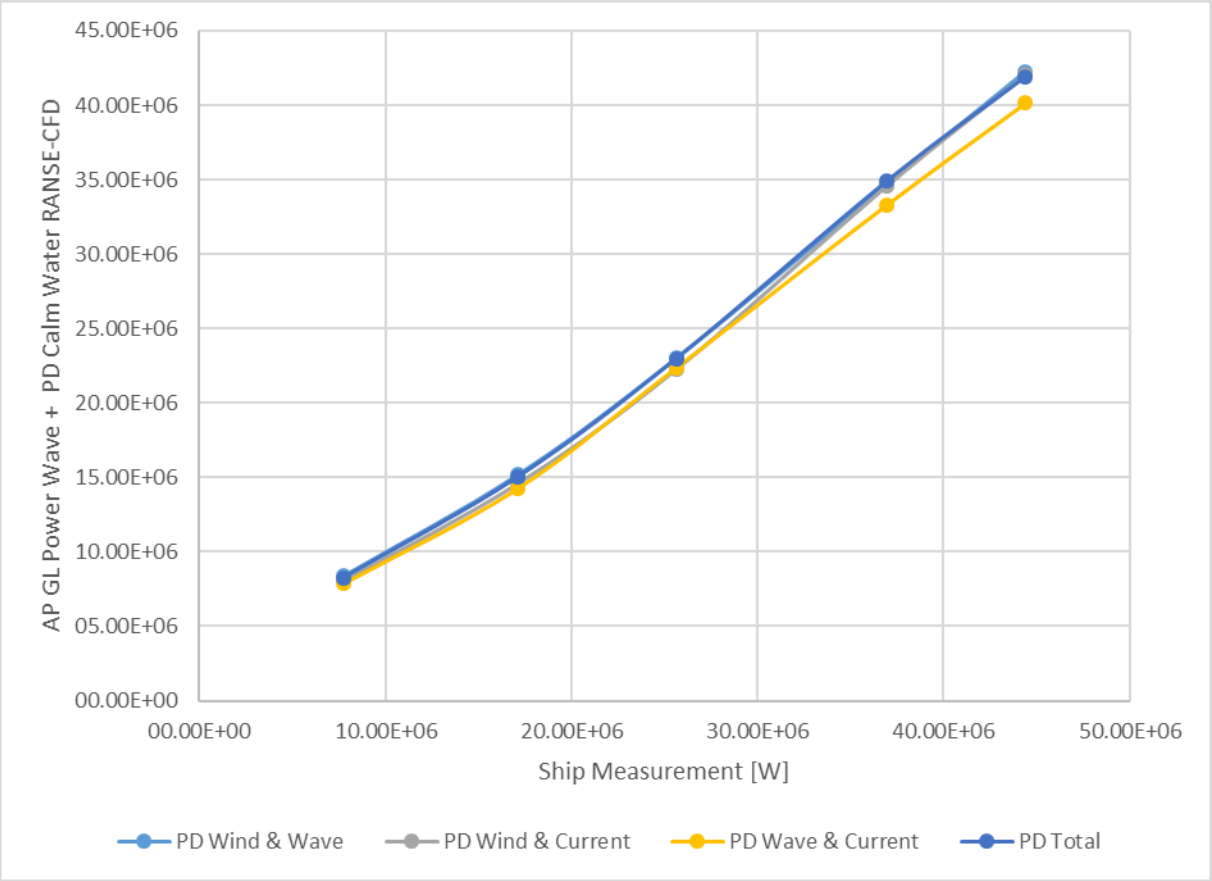


Figure 47 – Cases 5 to 8 - Distributed over shaft power.

Table 12 – Cases 1 to 4 average ratio by shaft power range.

| Range | | Average Ratio per Range | | | | |
|---|---|---|---|---|---|---|
| Shaft Power [kW] | | PD Calm Water (Case 1) | PD Wind (Case 2) | PD Wave (Case 3) | PD Current (Case 4) | PD Total Measured |
| min | 11.337 | 1,01 | 1,05 | 1,03 | 0,99 | 03,40E+06 |
| 11.337 | 21.372 | 0,82 | 0,86 | 0,84 | 0,81 | 07,26E+06 |
| 21.372 | 31.408 | 0,86 | 0,87 | 0,87 | 0,86 | 15,71E+06 |
| 31.408 | 41.443 | 0,89 | 0,93 | 0,90 | 0,90 | 25,10E+06 |
| 41.443 | max | 0,92 | 0,95 | 0,91 | 0,91 | 38,85E+06 |

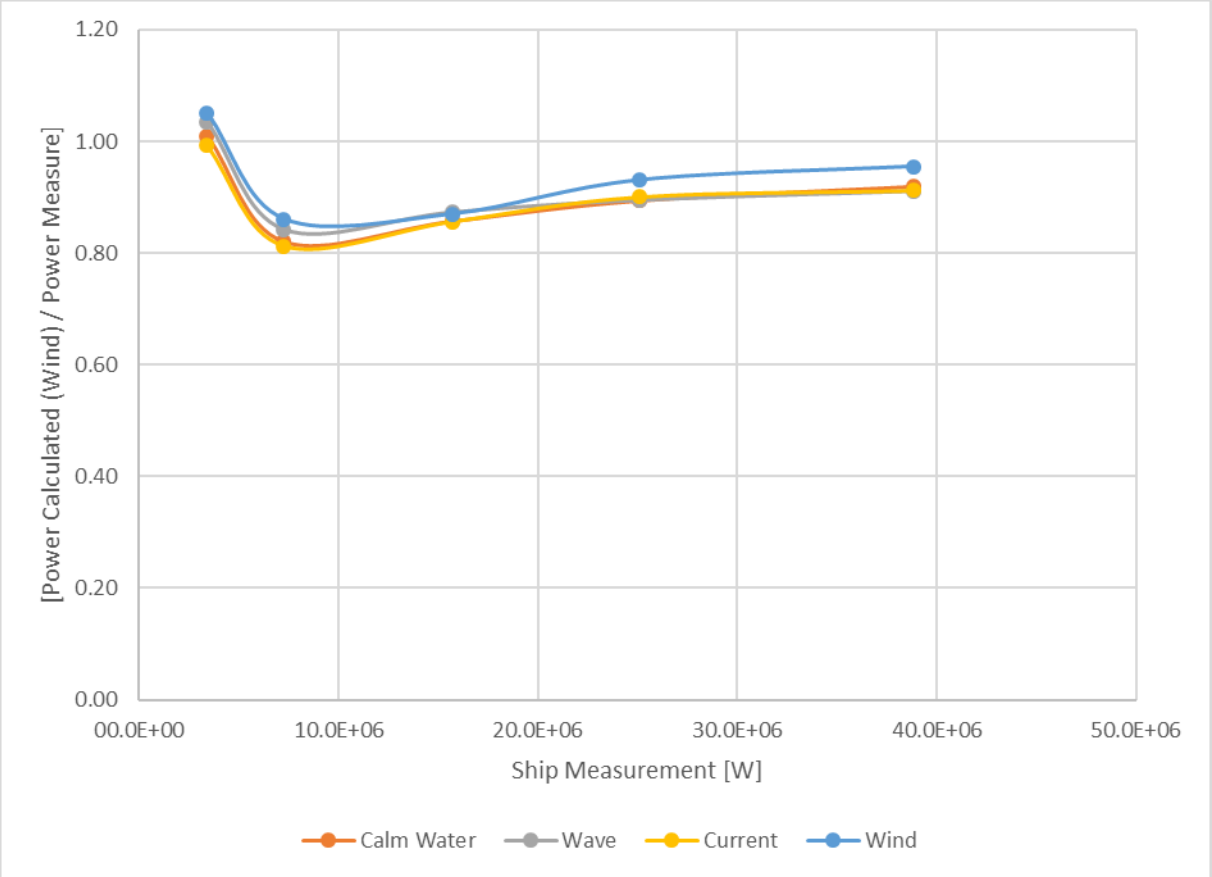


Figure 48 – Cases 1 to 4 ratio - distributed over shaft power.

Table 13 – Cases 5 to 8 average ratio by shaft power range.

| Range | | Average Ratio per Range | | | | |
|---|---|---|---|---|---|---|
| Shaft Power [kW] | | PD Wind & Wave (Case 5) | PD Wind & Current (Case 6) | PD Wave & Current (Case 7) | PD Total Calculated (Case 8) | PD Total Measured |
| min | 11.337 | 1,08 | 1,04 | 1,02 | 1,07 | 03,40E+06 |
| 11.337 | 21.372 | 0,89 | 0,85 | 0,83 | 0,88 | 07,26E+06 |
| 21.372 | 31.408 | 0,90 | 0,87 | 0,87 | 0,90 | 15,71E+06 |
| 31.408 | 41.443 | 0,94 | 0,94 | 0,90 | 0,94 | 25,10E+06 |
| 41.443 | max | 0,95 | 0,95 | 0,90 | 0,94 | 38,85E+06 |

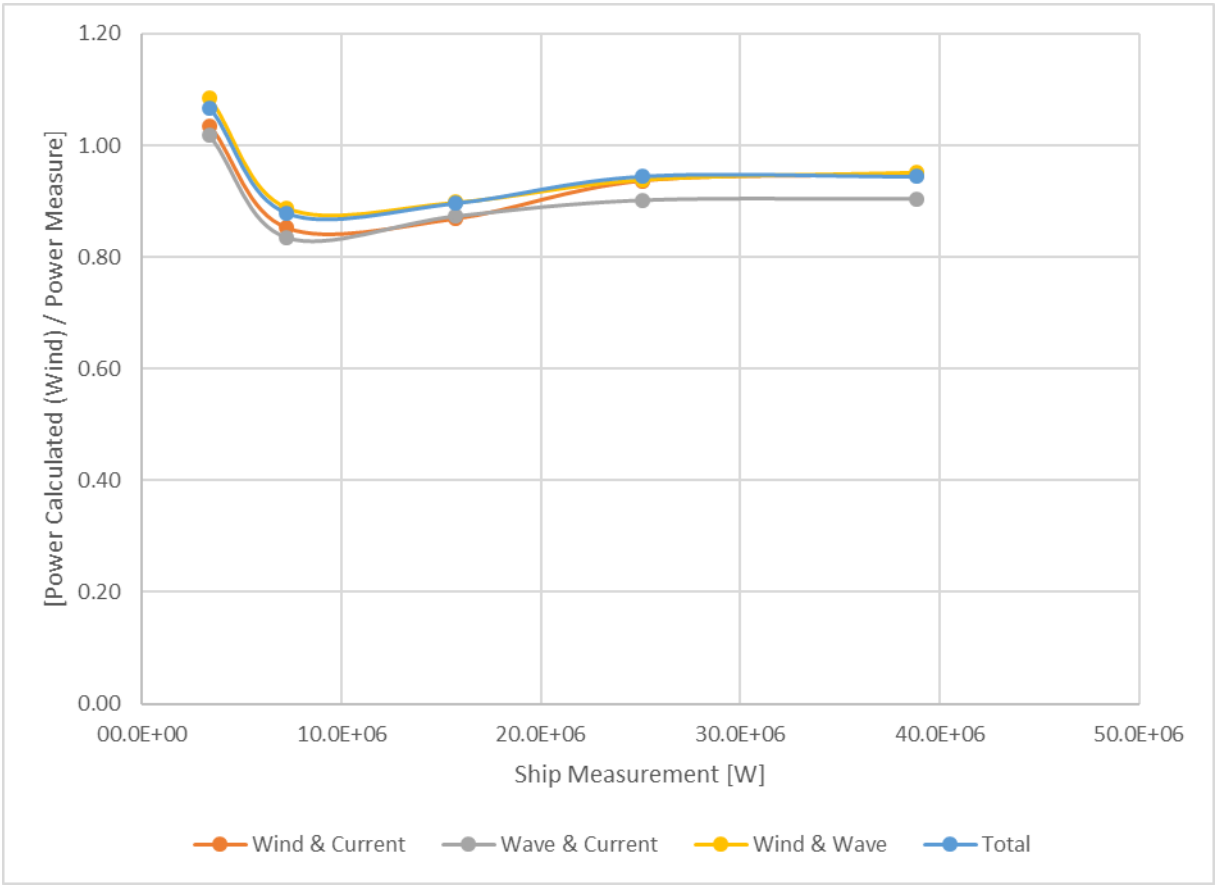


Figure 49 – Cases 5 to 8 Ratio - Distributed over shaft power.

Finally, from this set of analyses it is possible to see that the varying behavior that occurred on both previous studies has repeated in the above results. Nonetheless, the results for the most common shaft operating power showed that the order of influencing parameter on total power are: wave, wind and current.

# 6. CONCLUSION AND OUTLOOK

As discussed in chapter 1, this work aims to contribute to the scientific community and industry in different ways as well as for different players. For DNV GL, as a starting point to further develop its advisory software and services; to ship owners that based on those results can better optimize the ship route; ship design offices and towing tank basins that would get some benefit from this study on deciding which considerations to take on the ship optimization; and, lastly, for the scientific community that lately has put a lot of effort to investigate the added resistance of ships in waves, which of course has the same source of research content to the added power in seaways.

Apart from the contributions where those results could be further applied, the main raised question to be investigated and proposed by the author was to identify and study the influence of the parameters that may influence on the added power of a ship in seaway.

From the literature, it is seen that the added power can be derived from forces and moments equilibrium, as per equations. (1) to (3). Moreover, the main parameters that could influence on the added power of a ship are: wind, wave, current and rudder. However, it was decided on this work to have a closer look only on the environmental parameters: wind, wave and current.

The environmental parameters considered by the author was as accurate as possible, based on datasets provided by ERA-Interim and NASA (see Ref [6] and [8]). Although, the obtained data had some different grid mesh and measuring time steps differences, it was considered by the author that the usage of this source of information would provide more confidence on the obtained results believing that the magnitude of the values obtained and interpolated form those sources will be accurate enough to support the study.

Furthermore, a theoretical check on the influencing parameters were performed to get a first impression on the sensitive analysis study. From the theoretical results it was possible to see the importance of wind and wave together when compared by analyzing its $R^2$ value of 0.9771. Some further analyzing strategies were conducted aiming to better assess the results other than performing a linear regression fit.

Finally, to better visualize and compare the results, it was decided to average the scatter values dividing into sectors based on the ship speed and shaft power. The fluctuation of the results in regards to what is the most influencing parameter on the added power of a ship could lead for misinterpretations. Therefore, a histogram showing the most common operating ranges of the ship related to shaft RPM, ship speed and shaft power was considered to support the analyses.

The averaging results can be summarized on calculating the relative percent difference as shown in (28).

$$\frac{Power\ Calculated - Power\ Measured}{Power\ Measured} \tag{28}$$

From this expression, it is possible to visualize the most influencing parameter by checking the lowest values on the most common operation range. Those values are highlighted on Table 14 to Table 17.

Table 14 – Percent difference of influencing parameters on cases 1 to 4 – speed range.

| Range | | Average per range | | | |
|---|---|---|---|---|---|
| Speed [Knots] | | PD Calm Water (Case 1) | PD Wind (Case 2) | PD Wave (Case 3) | PD Current (Case 4) |
| Min | 13 | -14,7% | -6,1% | -12,5% | -12,3% |
| 13 | 16 | -29,3% | -28,2% | -25,3% | -28,6% |
| 16 | 19 | -22,2% | -19,3% | -20,8% | -21,9% |
| 19 | 22 | -12,1% | -10,6% | -10,6% | -12,3% |
| 22 | max | -4,7% | -0,1% | -4,9% | -5,4% |

Table 15 – Percent difference of influencing parameters on cases 5 to 8 – speed range.

| Range | | Average per range | | | |
|---|---|---|---|---|---|
| Speed [Knots] | | PD Wind & Wave (Case 5) | PD Wind & Current (Case 6) | PD Wave & Current (Case 7) | PD Total Calculated (Case 8) |
| Min | 13 | -4,0% | -3,7% | -10,1% | -1,6% |
| 13 | 16 | -24,0% | -27,5% | -24,7% | -23,4% |
| 16 | 19 | -17,0% | -19,0% | -20,5% | -16,7% |
| 19 | 22 | -8,0% | -10,8% | -10,8% | -8,2% |
| 22 | max | 0,2% | -0,8% | -5,6% | -0,5% |

Table 16 – Percent difference of influencing parameters on cases 1 to 4 – shaft power range.

| Range | | Average per range | | | |
|---|---|---|---|---|---|
| Shaft Power [kW] | | PD Calm Water (Case 1) | PD Wind (Case 2) | PD Wave (Case 3) | PD Current (Case 4) |
| Min | 11.337 | 1,0% | 5,1% | 3,5% | -0,7% |
| 11.337 | 21.372 | -17,9% | -14,0% | -15,7% | -18,8% |
| 21.372 | 31.408 | -14,3% | -13,0% | -12,6% | -14,4% |
| 31.408 | 41.443 | -10,6% | -6,9% | -10,5% | -10,0% |
| 41.443 | max | -8,1% | -4,5% | -8,9% | -8,8% |

Table 17 – Percent difference of influencing parameters on cases 5 to 8 – shaft power range.

| Range | | Average per range | | | |
|---|---|---|---|---|---|
| Shaft Power [kW] | | PD Wind & Wave (Case 5) | PD Wind & Current (Case 6) | PD Wave & Current (Case 7) | PD Total Calculated (Case 8) |
| Min | 11.337 | 8,4% | 3,5% | 1,7% | 6,8% |
| 11.337 | 21.372 | -11,2% | -14,8% | -16,6% | -12,1% |
| 21.372 | 31.408 | -10,2% | -13,1% | -12,7% | -10,3% |
| 31.408 | 41.443 | -6,1% | -6,3% | -9,8% | -5,5% |
| 41.443 | max | -4,8% | -5,3% | -9,6% | -5,6% |

From the results shown above and along the chapter 5, it is possible to conclude that wind plays an important whole on the total added power, being even greater than the added power due to waves. Nevertheless, the differences between those parameters aren't big enough to give a bigger emphasis to one or another. Therefore, the combined factors, wind and wave, should be considered the most important parameters that influence the ship added power in seaways.

# 7. FUTURE WORK AND FURTHER INVESTIGATIONS

Even though this thesis work has arrived to an end, the research has always room for improvement and further investigations. Therefore, a few proposals for the next steps on this topic are proposed as follows:

- Investigate the influence of Rudder on total added power.
- Investigate the influence of parameters for different environmental conditions directions.
- Perform this study for different types of ships.
- Investigate origin of the few outliers found on the work

# 8. ACKNOWLEDGEMENTS

This work would not be possible without the support and consideration of some persons and institutions. Thus, I would like to express my thankfulness to some of them.

Firstly, I would like to thank the support and attention of Prof. Philippe Rigo, coordinator of the EMSHIP program, Prof. Lionel Gentaz, coordinator of ECN program and Prof. Robert Bronsart, coordinator of URO, and all staff and universities part of EMShip program.

To my supervisor Dr. Ing. Vladimir Shigunov, who guided me through this research with enormous patience and kindness. Also, I am thankful to the colleagues that I've made in DNV GL Hamburg office, who supported me with personal and technical issued along this research.

My colleagues from DNV GL Rio de Janeiro Office that have supported me to enroll in this program, and in name of all of them, I would like to specially thank D.Sc. Marco Perez, that has proofed to be more than a workmate, but a great friend.

To my relatives in Brazil that with their positive vibrations and advices gave me strength to keep going even in tough times. To my grandfather José Muciano that is always there supporting and inspiring me to go after my dreams; and, to my godmother Vânia that the geographical proximity allowed her to be more present and assisting with all my family needs while in Europe.

To my beloved wife, who never stopped believing in me and to my daughter Giovanna and coming son Henrique. Definitely their presence next to me gave the necessary extra strength to conclude this journey.

Finally, I would like to thank God, which even in weak faith times, has never abandoned me and kept illuminating my life.

This thesis was developed in the frame of the European Master Course in "Integrated Advanced Ship Design" named "EMSHIP" for "European Education in Advanced Ship Design", Ref.: 159652-1-2009-1-BE-ERA MUNDUS-EMMC.

# 9. REFERENCES

[1]. Shigunov, V, 2017. Added Power in Seaway, *Ship Technology Research*, 64 (2), 65 – 75.

[2]. Alexandersson, M., 2009, *A study of methods to predict added resistance in waves*, Thesis (Master). KTH, Stockholm

[3]. NABERGOJ, R.; PRPIĆ-ORŠIĆ, J. (2007), A comparison of different methods for added resistance prediction, 22nd Int. Workshop Water Waves and Floating Bodies, Plitvice

[4]. N. VITALI; J. PRPIĆ-ORŠIĆ; C. GUEDES SOARES;(2016) Uncertainties related to the estimation of added resistance of a ship in waves, MARTECH

[5]. YUTA SEKI; MASASHI KASHIWAGI; HIDETSUGU IWASHITA, Experimental study on added resistance and unsteady pressure distribution in following waves, Proceedings of PRADS2016 September, 2016

[6]. Lakshmynarayanana, P. A., Hudson, D. A., 2017. Estimating Added Power in Waves for Ships Through Analysis of Operational Data. *In*: V. Bertram, ed. *2nd Hull Performance & Insight Conference*. Ulrichshusen: HullPIC'17, 253 – 263.

[7]. Bonjean, F., and G. S. E. Lagerloef, 2002. Diagnostic model and analysis of the surface currents in the tropical Pacific Ocean. *J. Phys. Oceanogr.* 32, 2938-2954.

[8]. Dee, D. P., Uppala, S. M., Simmons, A. J., Berrisford, P., Poli, P., Kobayashi, S., Andrae, U., Balmaseda, M. A., Balsamo, G., Bauer, P., Bechtold, P., Beljaars, A. C. M., van de Berg, L., Bidlot, J., Bormann, N., Delsol, C., Dragani, R., Fuentes, M., Geer, A. J., Haimberger, L., Healy, S. B., Hersbach, H., Hólm, E. V., Isaksen, L., Kållberg, P., Köhler, M., Matricardi, M., McNally, A. P., Monge-Sanz, B. M., Morcrette, J.-J., Park, B.-K., Peubey, C., de Rosnay, P., Tavolato, C., Thépaut, J.-N. and Vitart, F., 2011. The ERA-Interim reanalysis: configuration and performance of the data assimilation system. *Q.J.R. Meteorol. Soc*, 137 (656), 553–597.